Introduction to Neutron Radiography and Computed Tomography

Hassina Bilheux

Neutron Imaging Scientist
Cellphone #: 865-384-9630

June 19th, 2019

Neutron School Team:
Shawn Zhang
Jean Bilheux
Hassina Bilheux

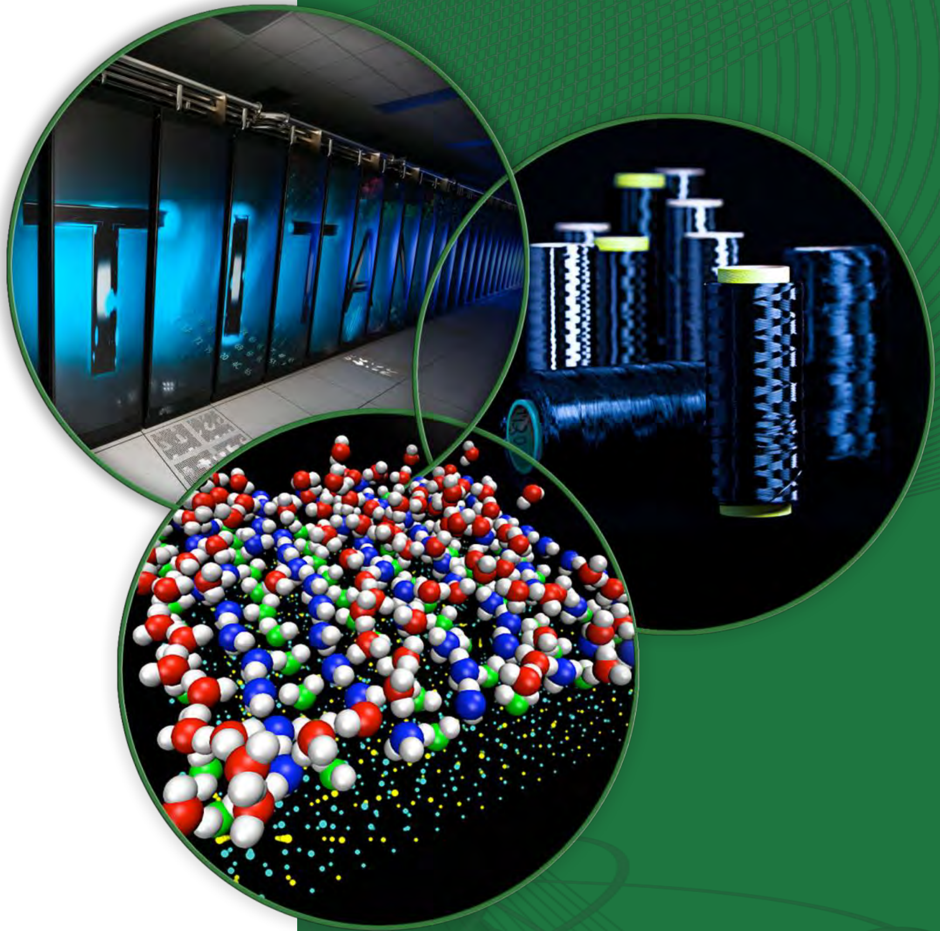

ORNL is managed by UT-Battelle
for the US Department of Energy

OAK RIDGE
National Laboratory

Imaging is a Growing Part of the ORNL Neutron Sciences Program

High Flux Isotope Reactor (HFIR)
Intense steady-state neutron flux and a high-brightness cold neutron source

Spallation Neutron Source (SNS)
rful
eutron

Dedicated Imaging Instrument (CG-1D)
Steadily improving capabilities
Expanded support

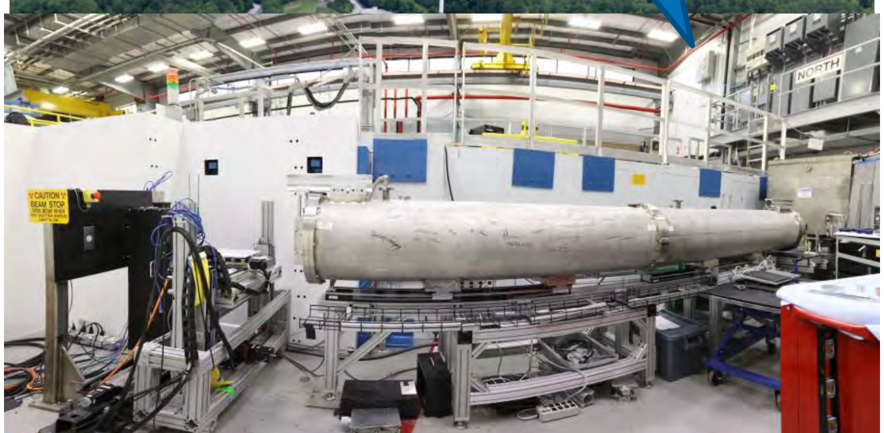

Techniques such as Bragg-edge imaging are being implemented on BL3 SNAP diffractometer (VENUS is the future imaging beamline)

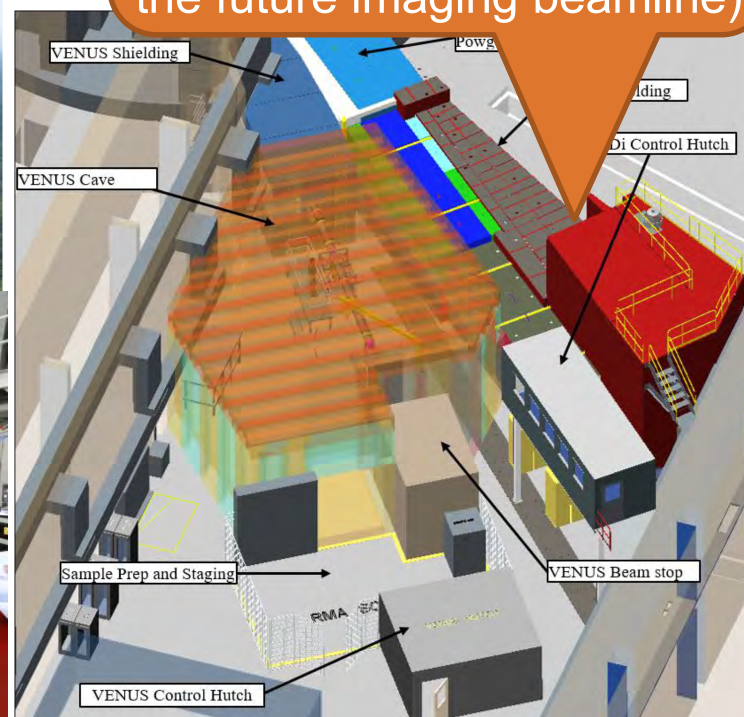

Neutrons Measure Structure and Dynamics

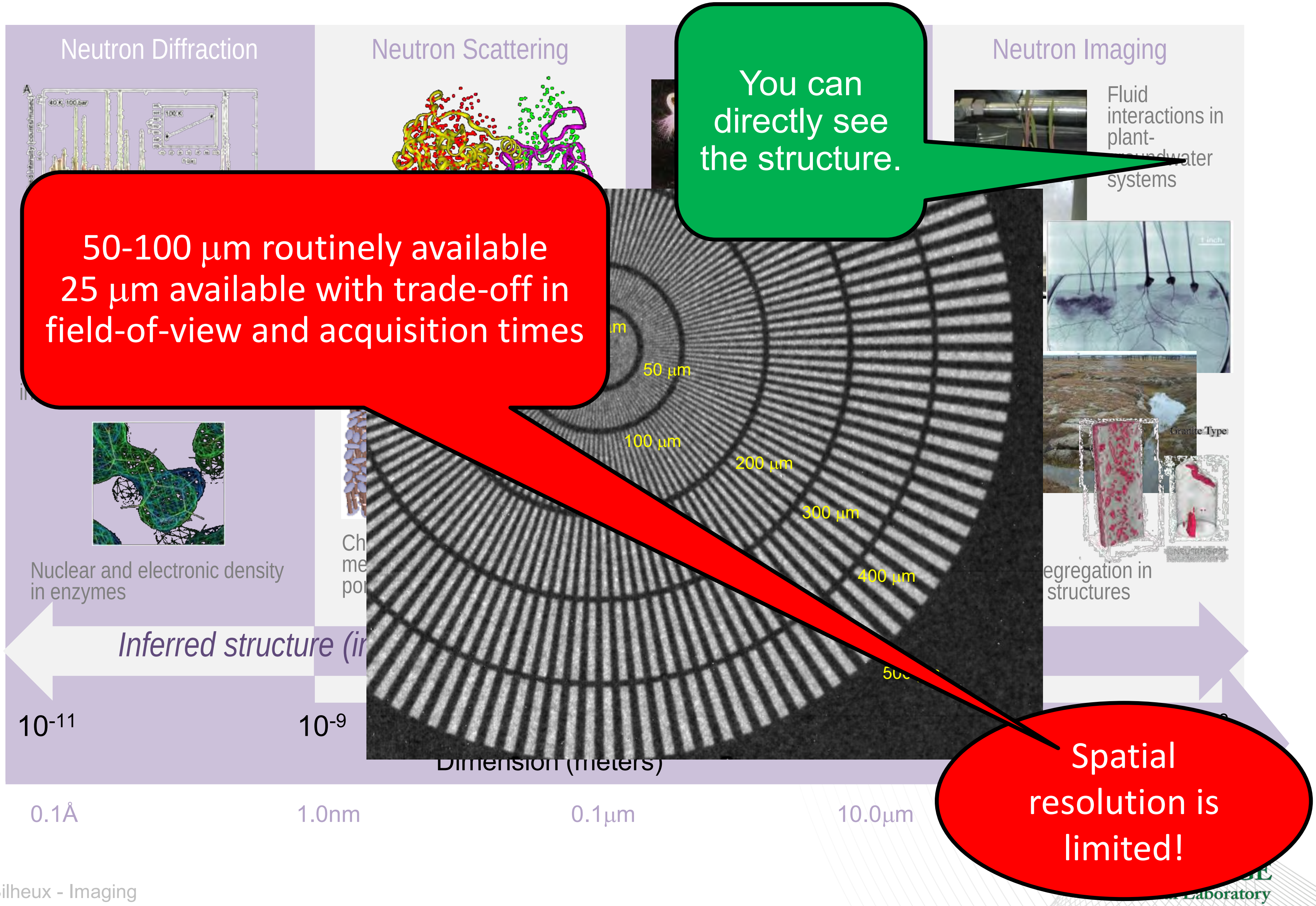

Neutrons can detect light elements such as H buried in heavy elements such as Fe

Isotope Sensitivity (important for soft matter studies)

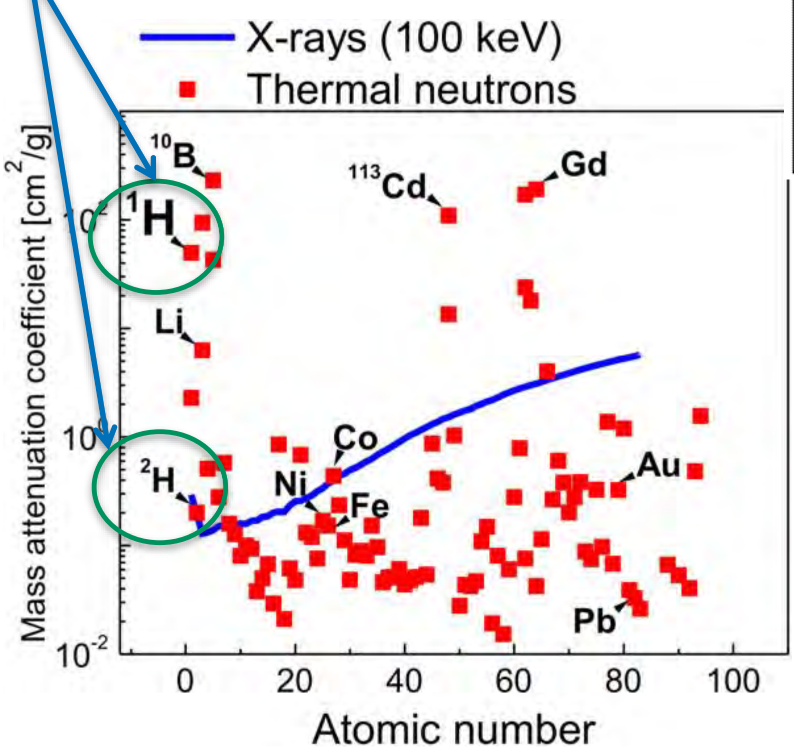

*[M. Strobl et al., J. Phys. D: Appl. Phys. **42** (2009) 243001]*

Neutron *Radiograph* ***X-ray*** *Radiograph*

Courtesy of E. Lehmann,PSI

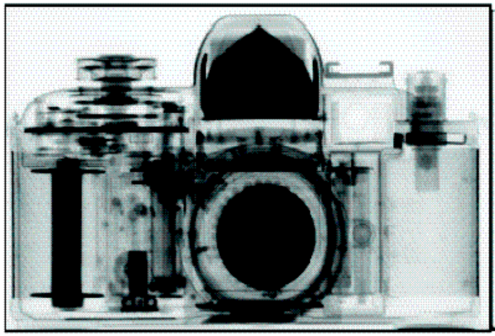

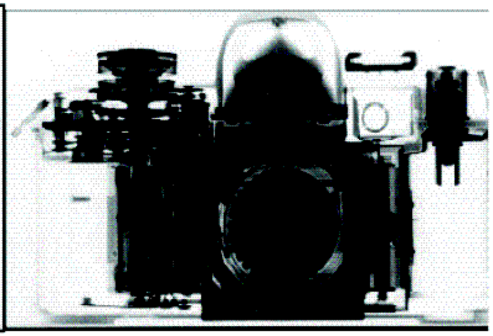

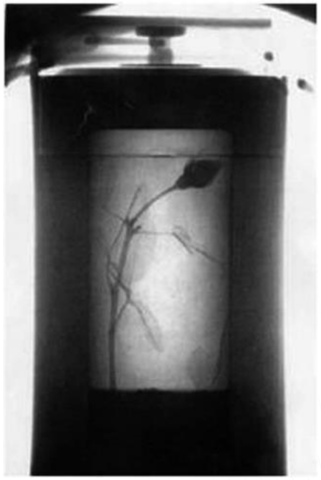

Neutron Radiograph *of Rose in Lead Flask*

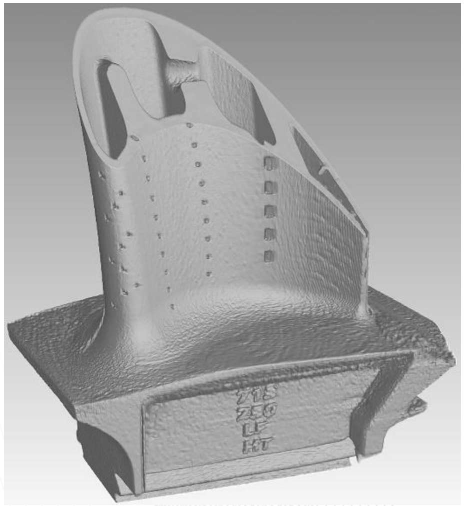

Neutron CT *of an Inconel Turbine Blade*

HFIR CG-1D Imaging has a broad scientific portfolio

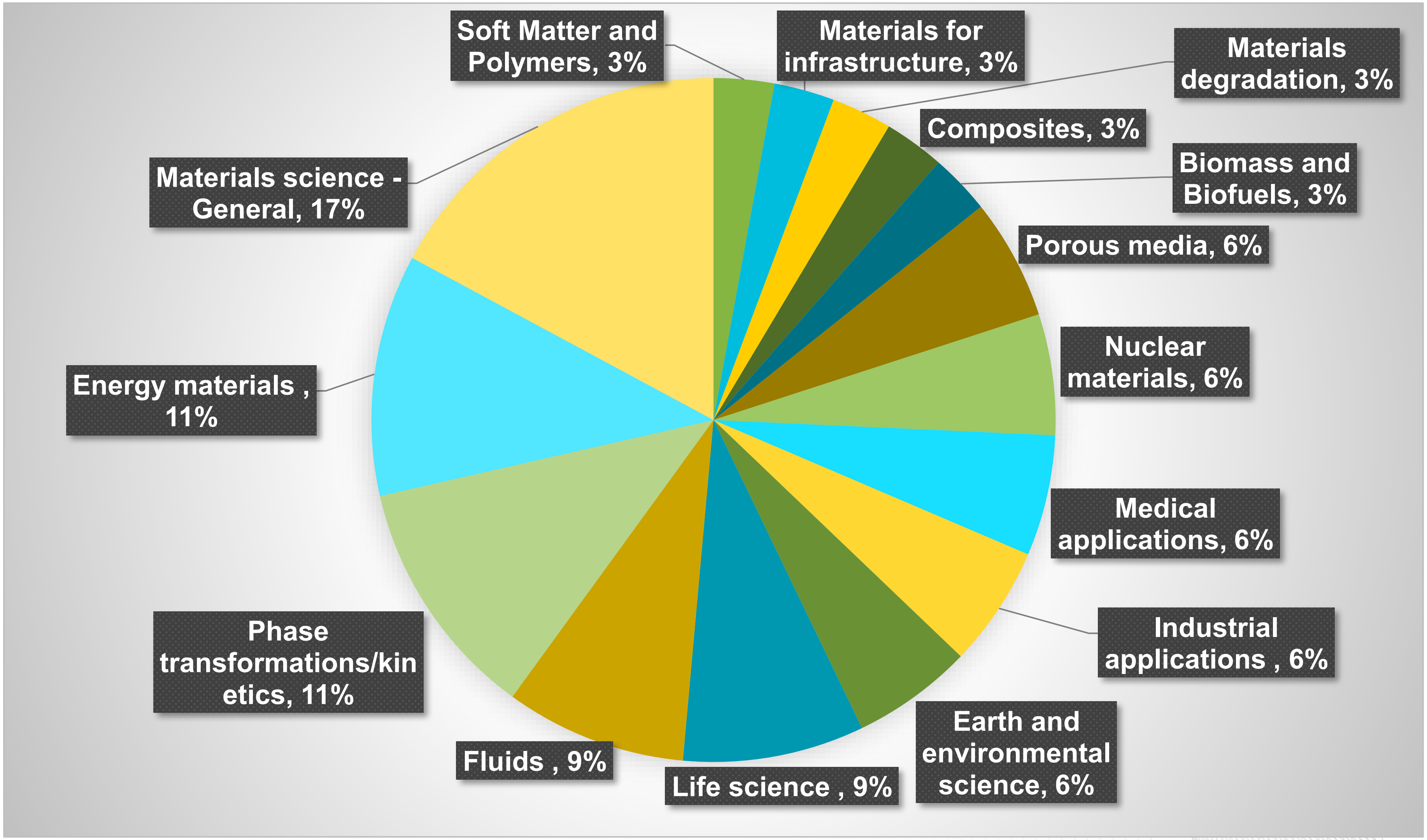

Neutron imaging supports applied research with academia, industry and government agencies

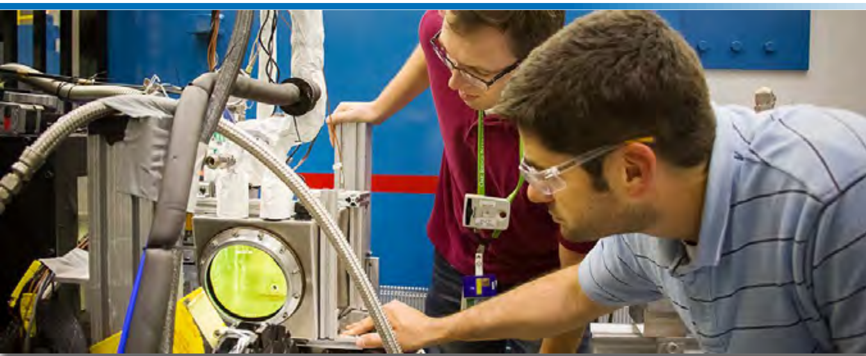

Game #1: Can you guess what this neutron radiograph represents?

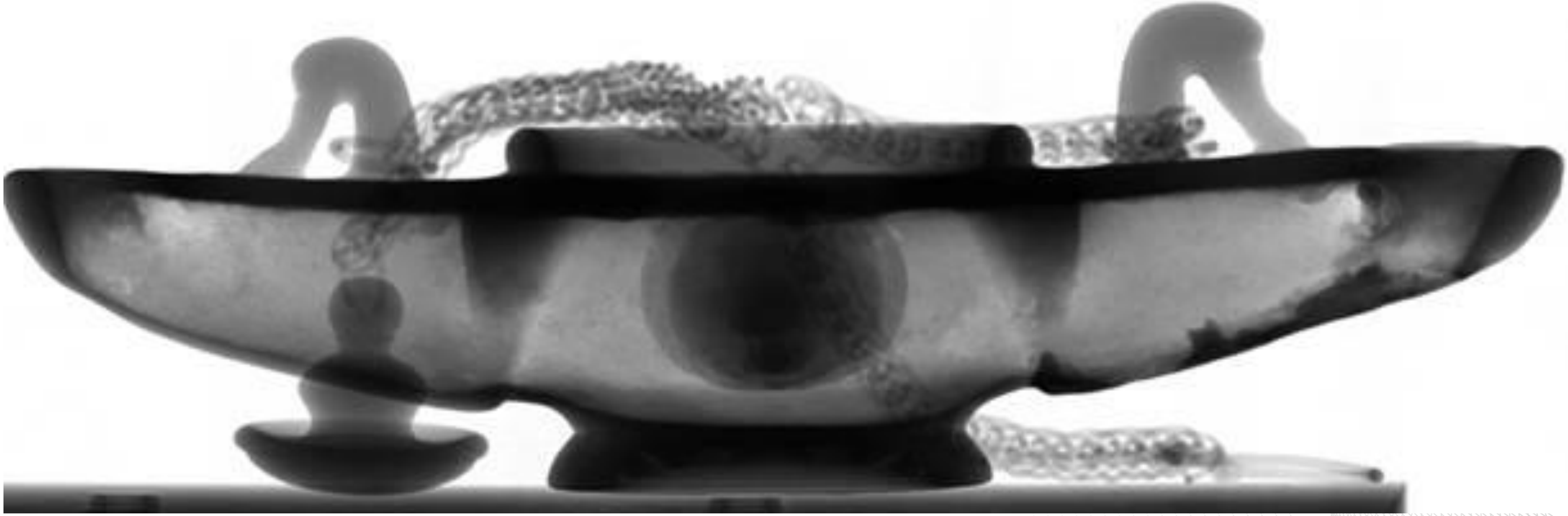

What is imaging?

- Imaging is the visual representation of an object: photography, cinematography, medical imaging, X-ray imaging, thermal imaging, molecular imaging, neutron imaging, etc.

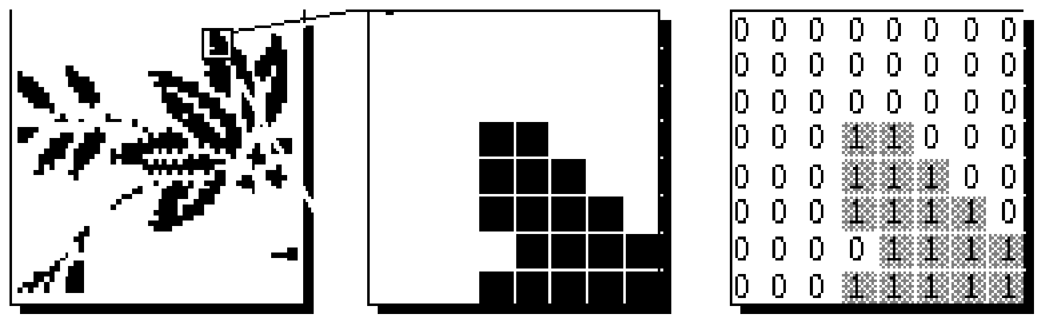

- Digital Imaging is a field of computer science covering images that can be stored on a computer as *bit-mapped* images

Image Modalities and Imaging Science & Technology throughout Nobel Prize history

- 1901: Roentgen, FIRST Nobel Prize in Physics,
  Discovery of X-rays
- 1932: Chadwick, Nobel Prize in Physics
  Discovery of Neutrons
- 1979: Cormack and Hounsfield, Nobel Prize in Medicine, Computed Tomography (CT)
- 1986: Ruska, Binnig, Rohrer, Nobel Prize in Physics,
  Electron Microscopy
- 2003: Lauterbur and Mansfield, Nobel Prize in Medicine, Magnetic Resonance Imaging (MRI)
- 2009: Boyle and Smith, Nobel Prize in Physics,
  Imaging semi-conductor circuit, the CCD* sensor
- (*) Charge-Coupled Device

Early neutron imaging measurements

- **Neutron Imaging started in the mid 1930's but only during the past 30** years has it come to the forefront of non-destructive testing

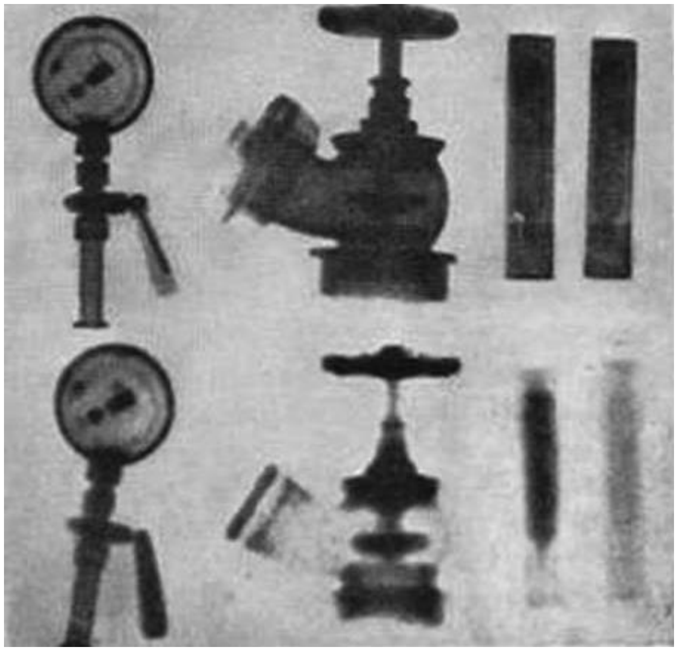

Discovery of neutron in 1932 by Chadwick

First neutron radiograph in 1935

Left to right: Pressure gauge with metal backplate; fire hydrant and test tubes filled with H_2O
and D_2O imaged with gamma-rays (top) and neutrons (bottom)
[Kallman and Kuhn, Research 1, 254 (1947)]

- Dedicated world class imaging user facilities such as NIST, PSI, HZB, FRM-II, J-PARC and at many worldwide universities
- World conferences and workshops being held regularly
- Growing worldwide user community

Multiple scattering and low detector spatial resolution

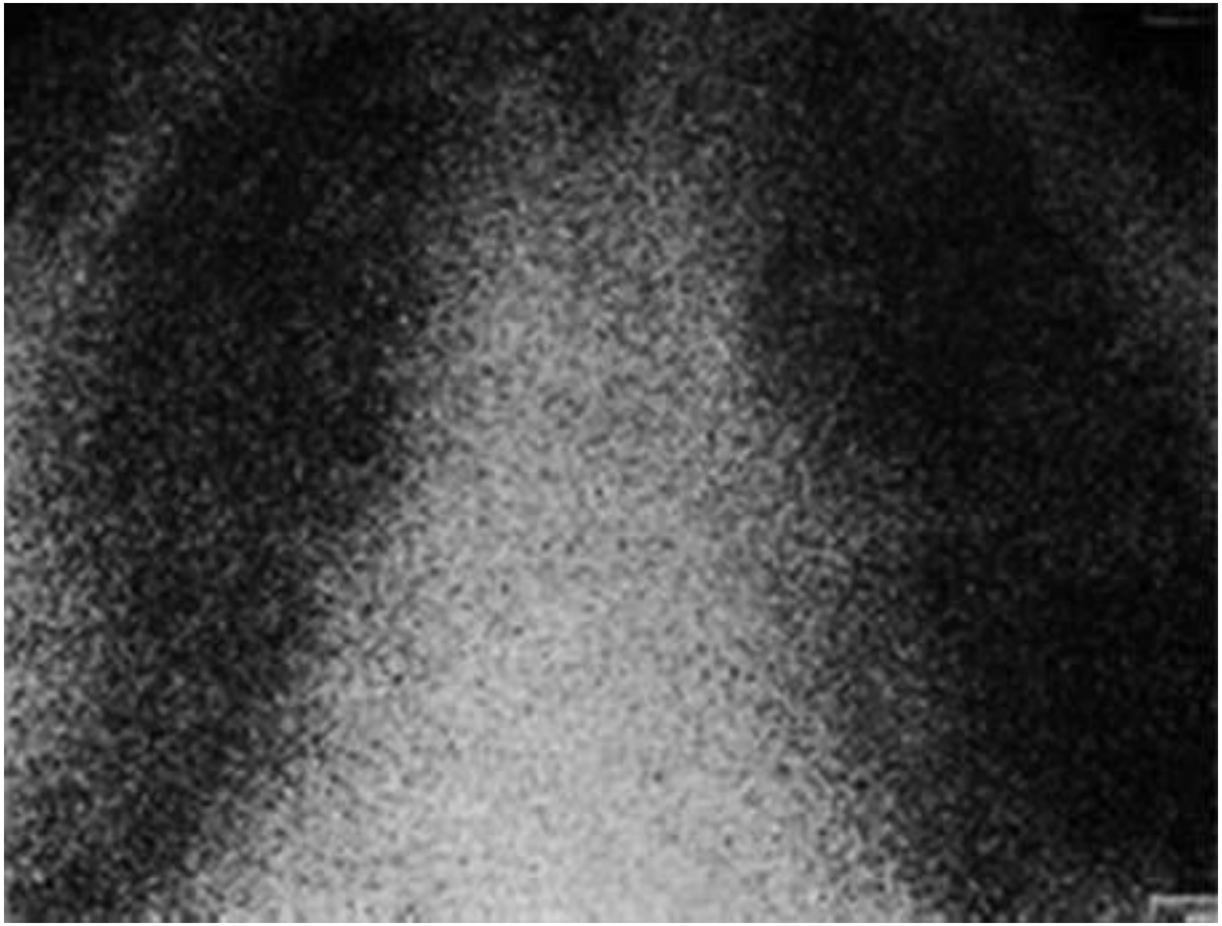

[J. Anderson et al., Br. J. Radiol. 37, 957 (1964)]

Today: Comparison microscopy/microCT and neutron radiography

Microscope

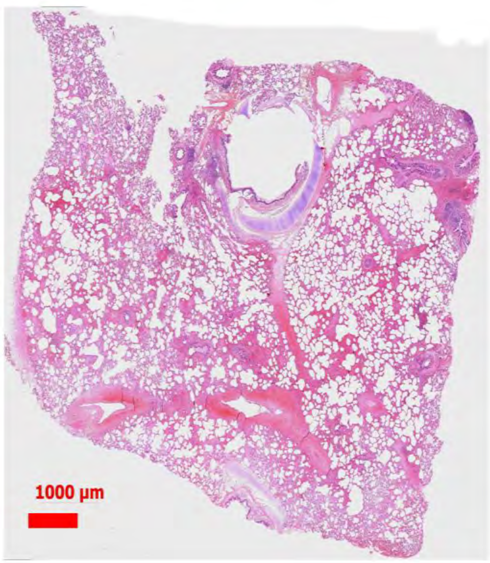

microCT

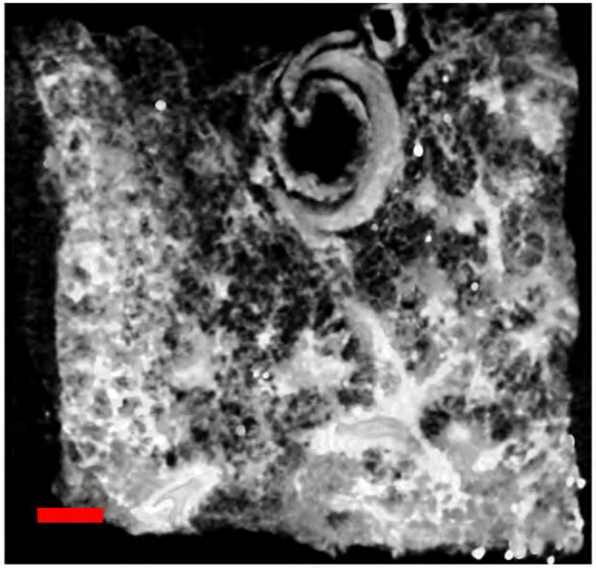

Neutron

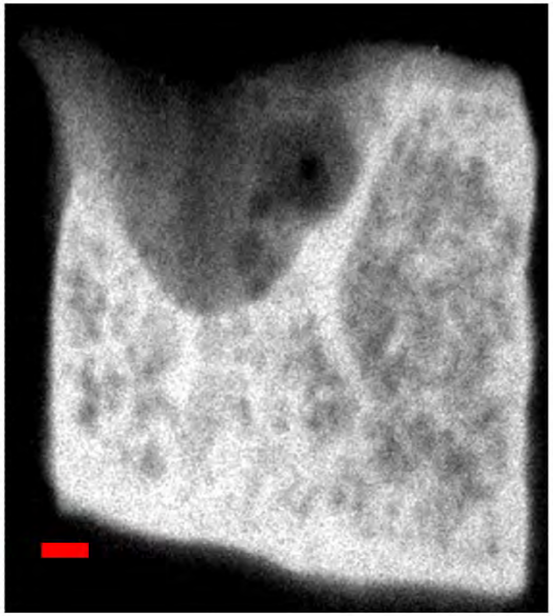

- 92% of the pixel intensities agreement between histological and neutron

Watkin, K. et al., Neutron Imaging and Applications, Springer, 2009.

Quantitative Neutron Imaging

Lambert-Beer Law:

$$T = \frac{I(\lambda)}{I_0(\lambda)} = e^{-\mu(\lambda)\Delta x}$$

μ is the attenuation coefficient and Δx is the thickness of the sample

$$\mu(\lambda) = \sigma_t(\lambda)\frac{\rho N_A}{M}$$

$\sigma_t(\lambda)$ is the material's total cross section for neutrons, ρ is its density, N_A is Avogadro's number, and M is the molar mass.

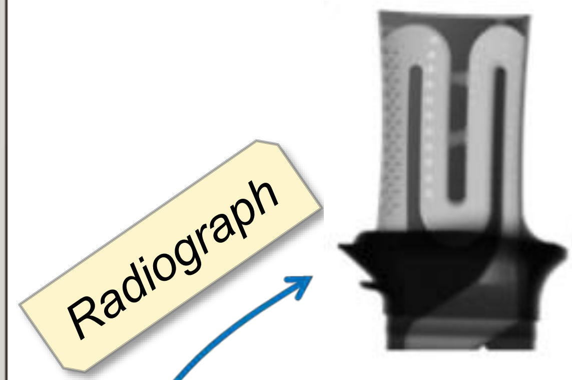

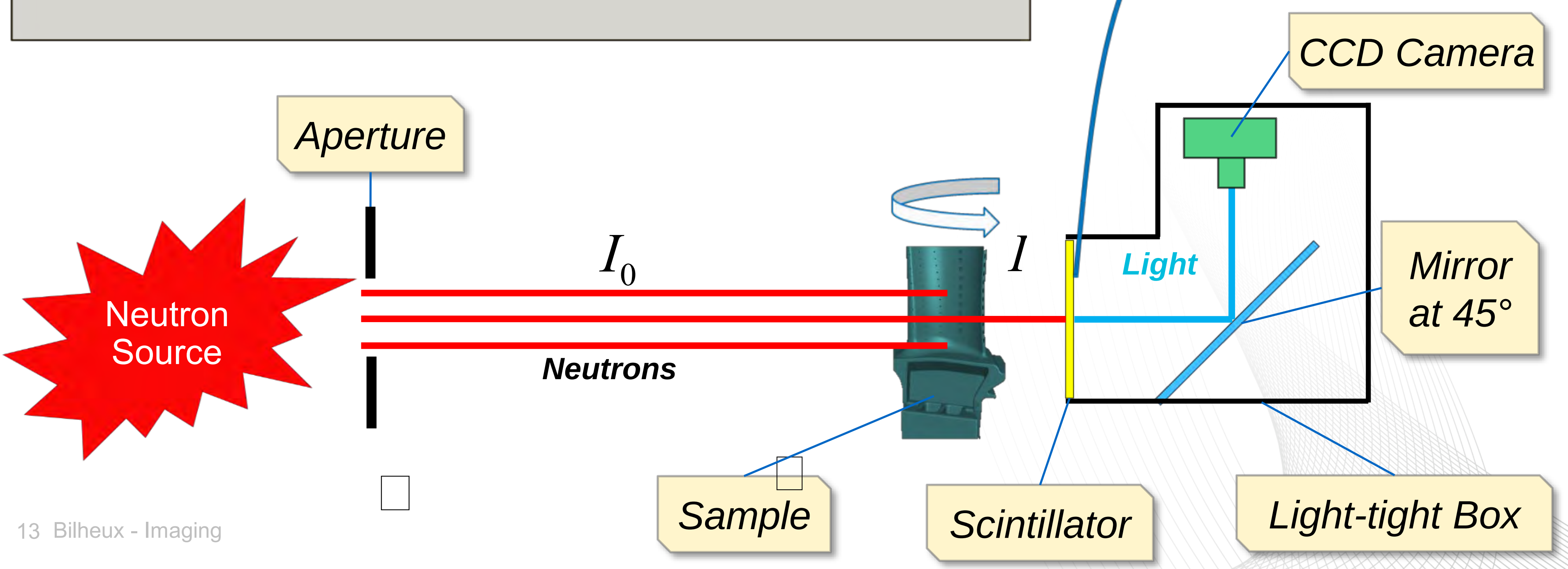

Data Normalization for Imaging

- 2D – Radiography
  - Normalization

$$I_N(i,j) = \frac{I(i,j) - DF(i,j)}{OB(i,j) - DF(i,j)}$$

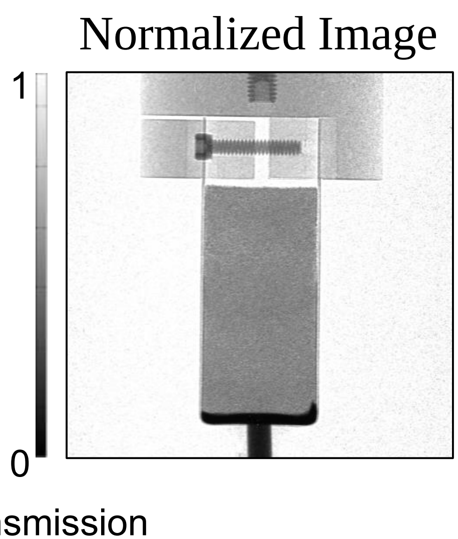

=

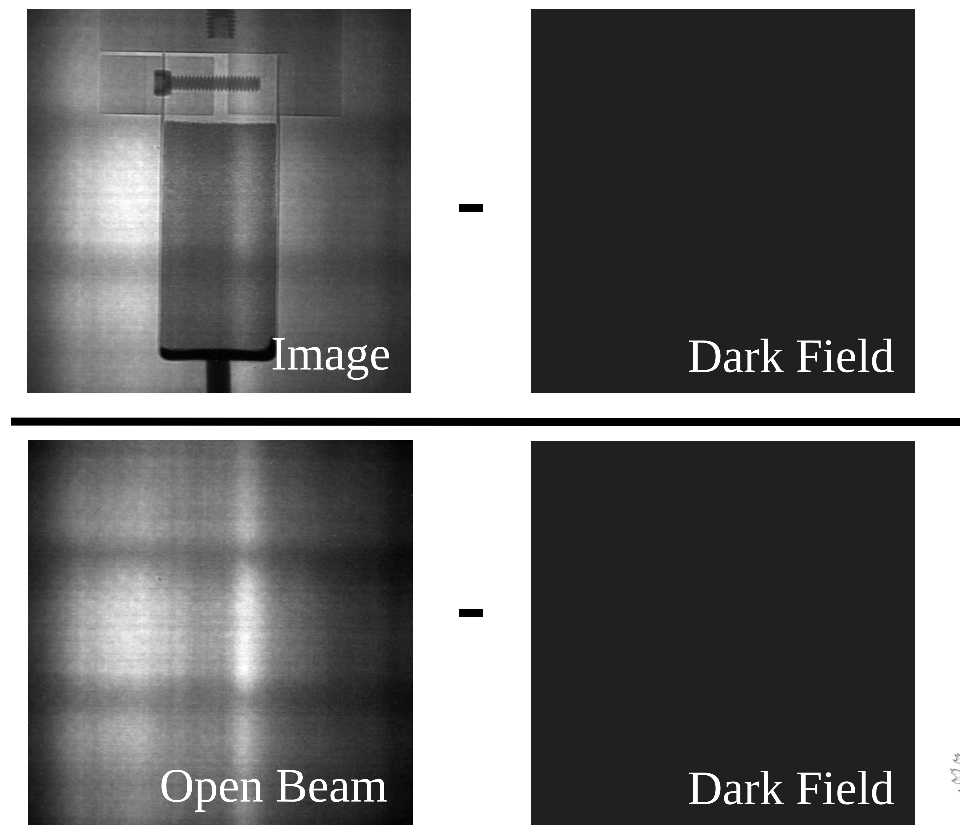

Computed/Computerized Tomography (CT)

- Several techniques:
  - Filtered Back Projection
    - Radon transform
    - Works well with high signal to noise ration measurements
    - Easy-to-use commercial, semi-automated software available
    - Quick
  - Iterative Reconstruction
    - Direct approach
    - Less artifacts
    - Can reconstruct incomplete data
    - High computation time

Computed/Computerized Tomography (Filtered Back Projection)

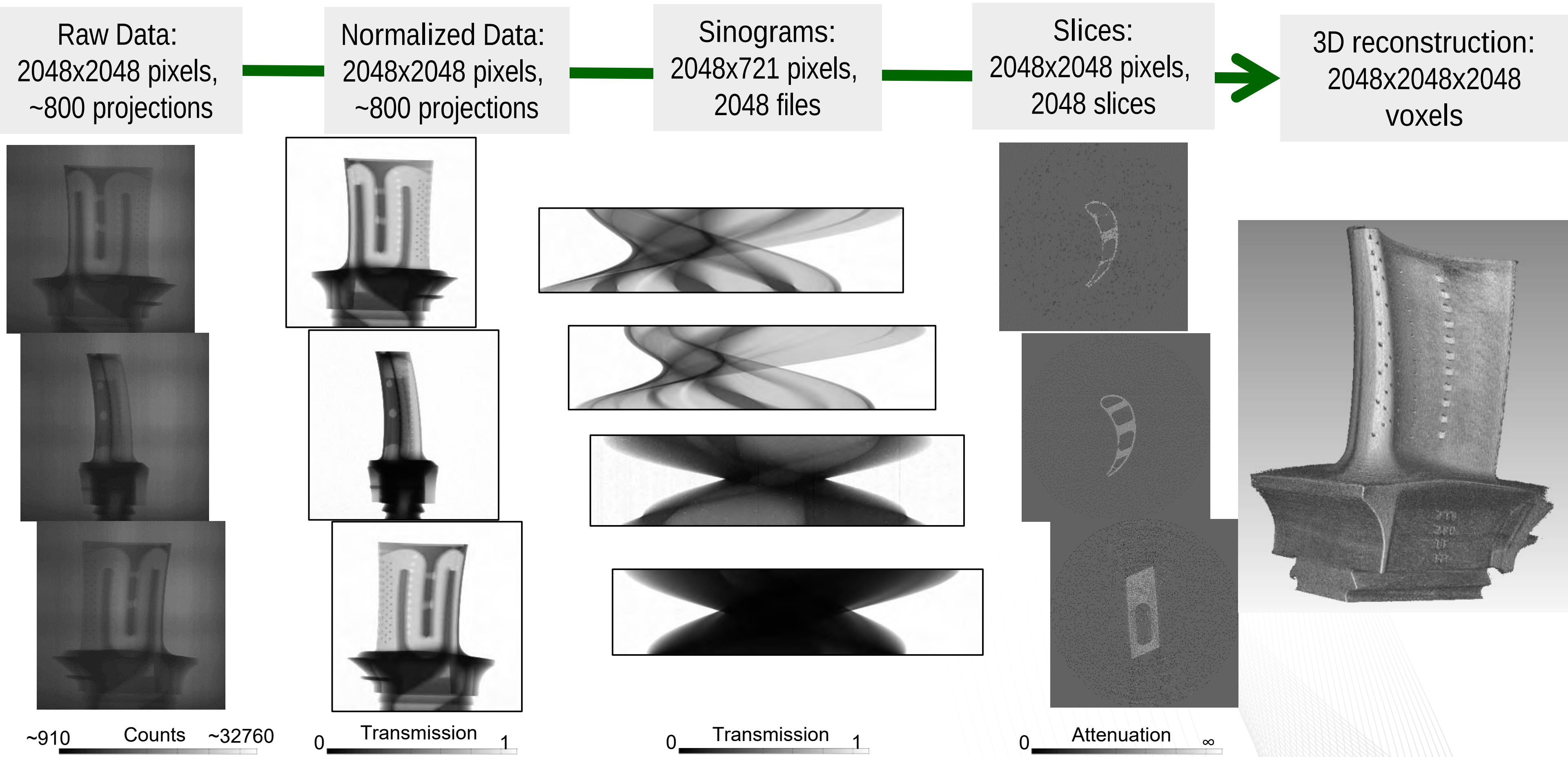

Turbine Blade CT Video
available here

Detection of “imaging” neutrons

- Scintillator-based techniques such as $^{6}Li(n,\alpha)\ ^{3}H$
  - Good signal-to-noise (SNR) ratio
  - Large Field Of View (FOV) and 0.01 to hundreds of seconds images
  - BUT spatial resolution limited by the dissipation of particles
  - Can take a lot of neutron flux!

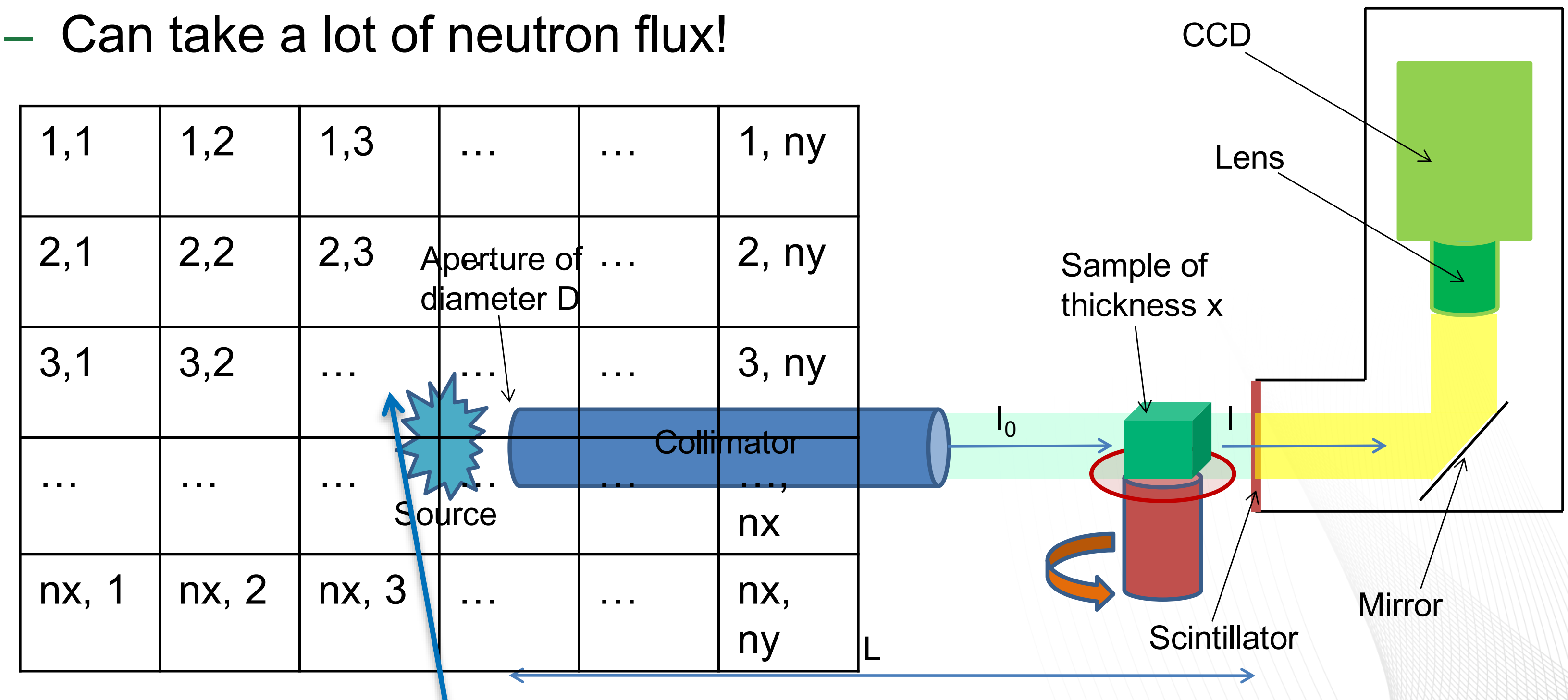

Each pixel is coded using n-bit.
16-bit = pixel value is between 0 and 65535

Detection of “imaging” neutrons (cont’d)

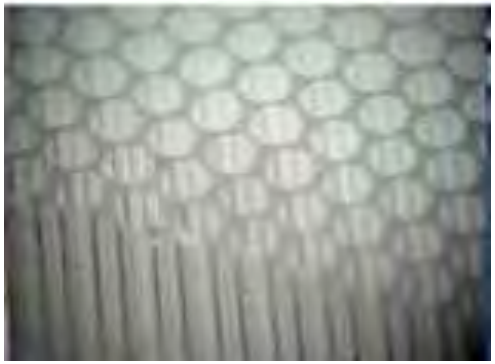

Courtesy of Prof. A. Tremsin, UC-Berkeley

- Pixelated detectors
  - Micro-Channel Plate (MCP)
  - In the direct path of the beam
  - Limited FOV for high spatial resolution MCPs
    - 1.4 cm x 1.4 cm at ~ 15 microns
  - Encodes events at x, y position and time of arrival, at high temporal resolution ~ 1 MHz
  - Detection efficiency has improved for both cold (~70%) and thermal (~50%) energy range
  - Absence of readout noise
  - Not as gamma sensitive
  - Becoming commercial
  - BUT: works in relatively low-signal beam!

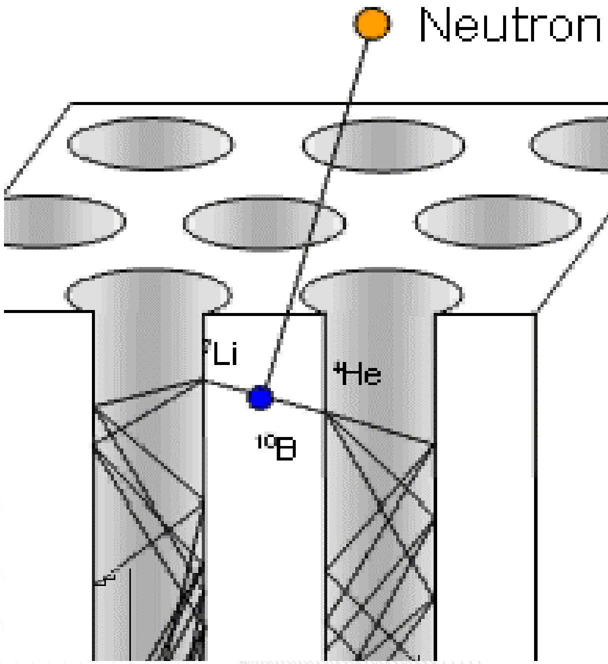

http://www.novascientific.com/neutron.html

CG-1D: Cold Neutron Imaging Beamline at HFIR

The CG-1D neutron imaging beamline is designed to probe **structural features** of length scales between **~ 25-100 µm** and a few mm and **kinetic changes** on time scales between a few µs (repetitive motion events) to hours across a wide variety of subjects (e.g., batteries, engineering components, geological systems, biological systems, archeology and condensed matter).

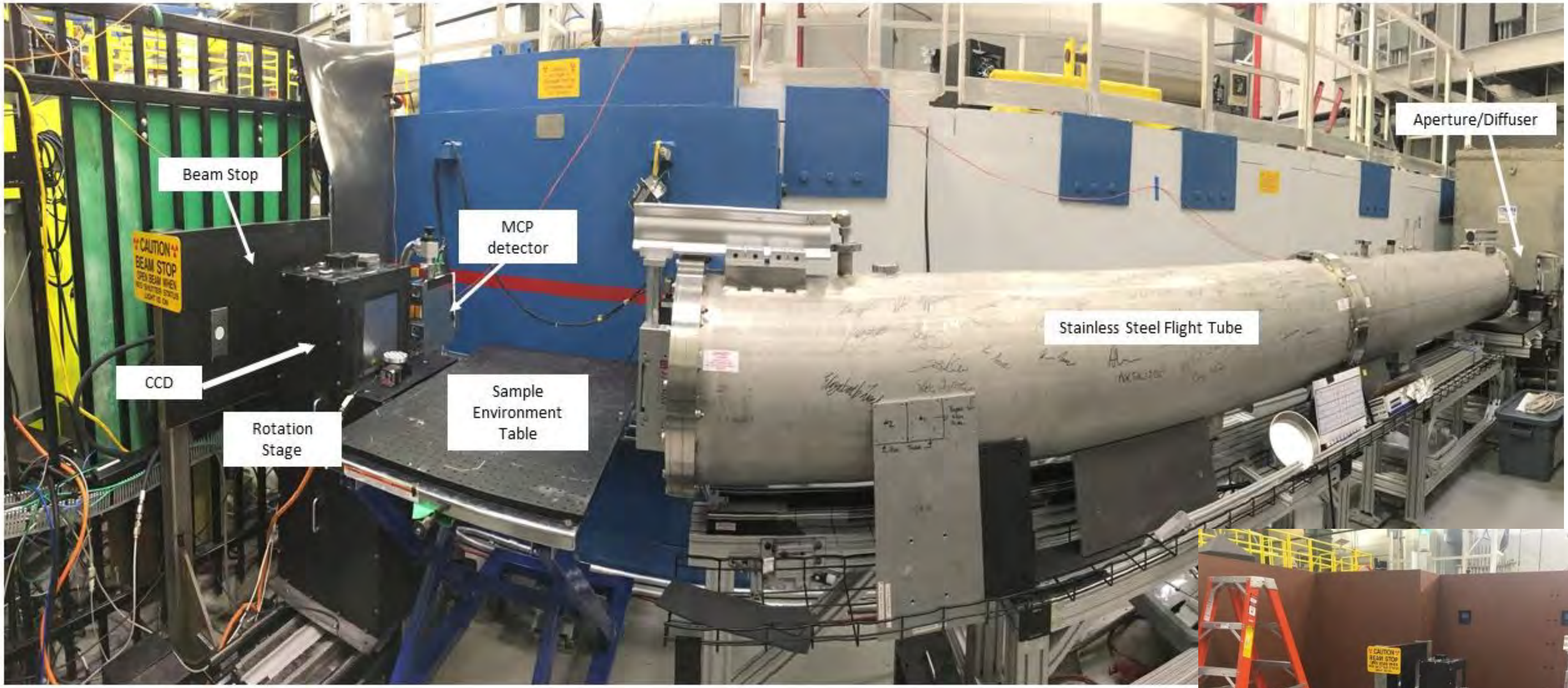

CG-1D Neutron Imaging Facility (HFIR)

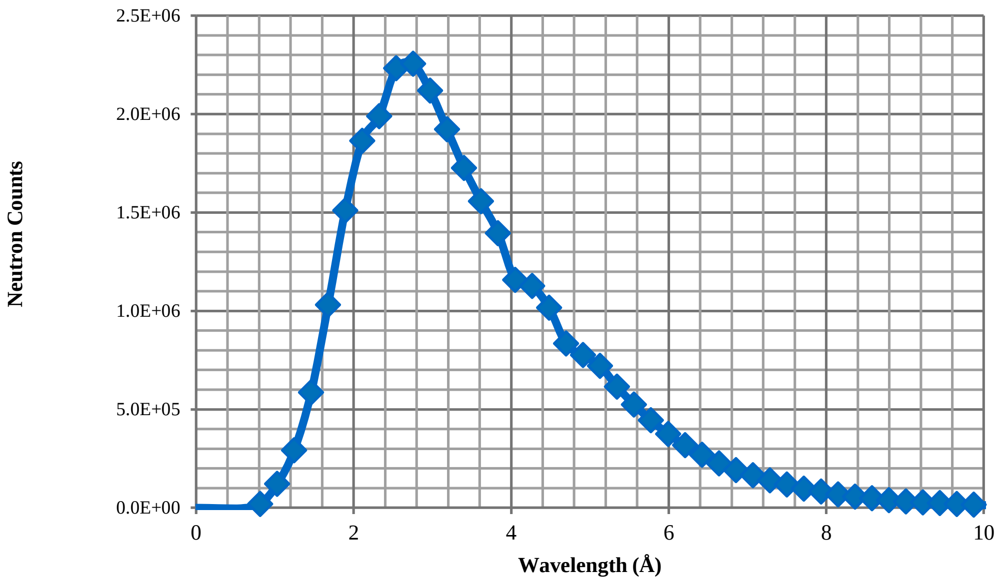

Neutron wavelength distribution at CG-1D

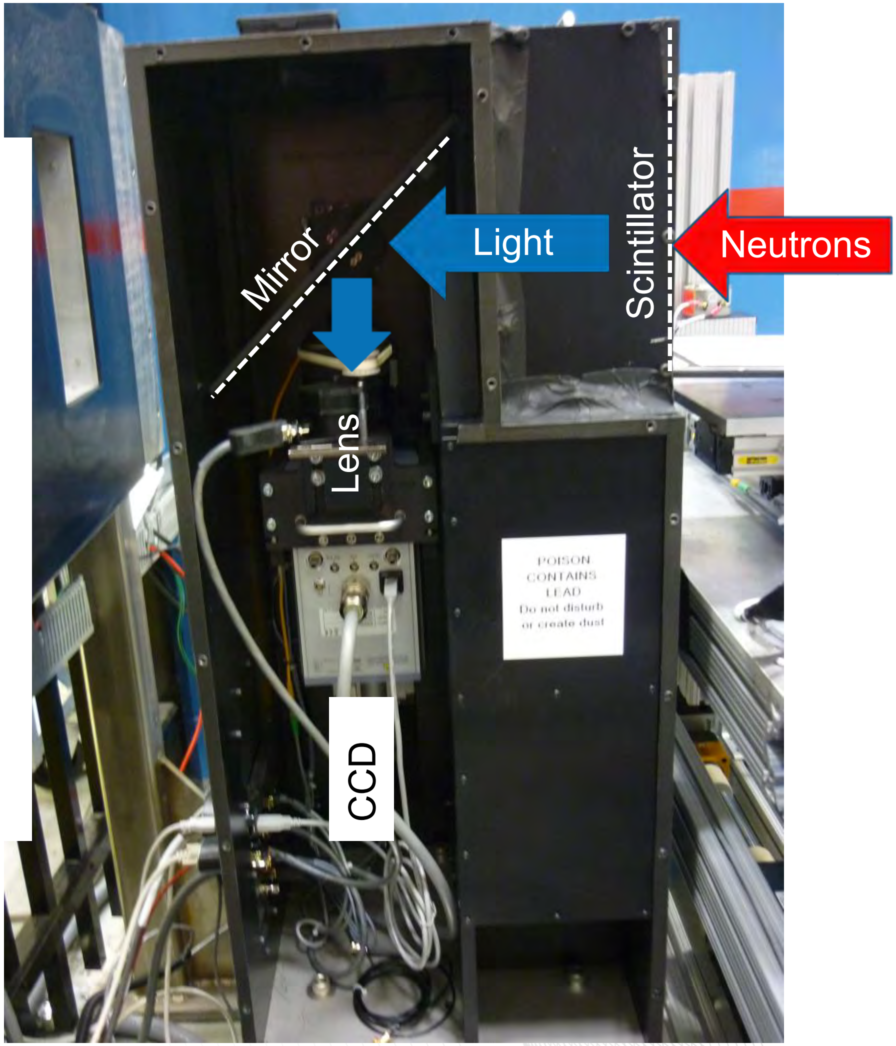

Detector assembly (side view)

OAK RIDGE
National Laboratory

Conventional Neutron Imaging Techniques at Steady-State (HFIR) Sources

- Radiography
- Tomography

Routinely available at CG-1D

- Stroboscopic Imaging
- Imaging of processes that happen fast

Available at CG-1D using the MCP detector

- Polarized Neutron Imaging
- Monochromatic Imaging

Newly implemented at CG-1D

- Grating Interferometry (Phase and Dark Field Imaging)
  - Under development
  - Increased spatial resolution and different contrast mechanism (less than 20 μm)

Neutron Imaging Techniques at pulsed sources (SNS)

- Wavelength-dependent (or Time-of-Flight) imaging
  - Contrast enhancement
  - Bragg edge
  - Resonance Imaging/Spectroscopy

  Available at SNS SNAP using the MCP detector
- Stroboscopic imaging
  - SNS has a natural clock
- Neutron Imaging at energies not accessible at reactor facilities
  - Mainly bio-medical applications

Resonance imaging allows isotopic mapping at the SNS

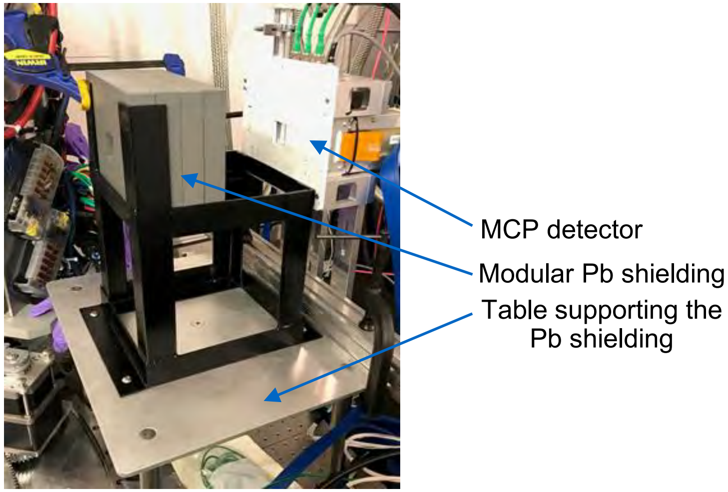

Photograph of the 4-in thick lead shielding and support table at the SNAP beamline with the MCP detector.

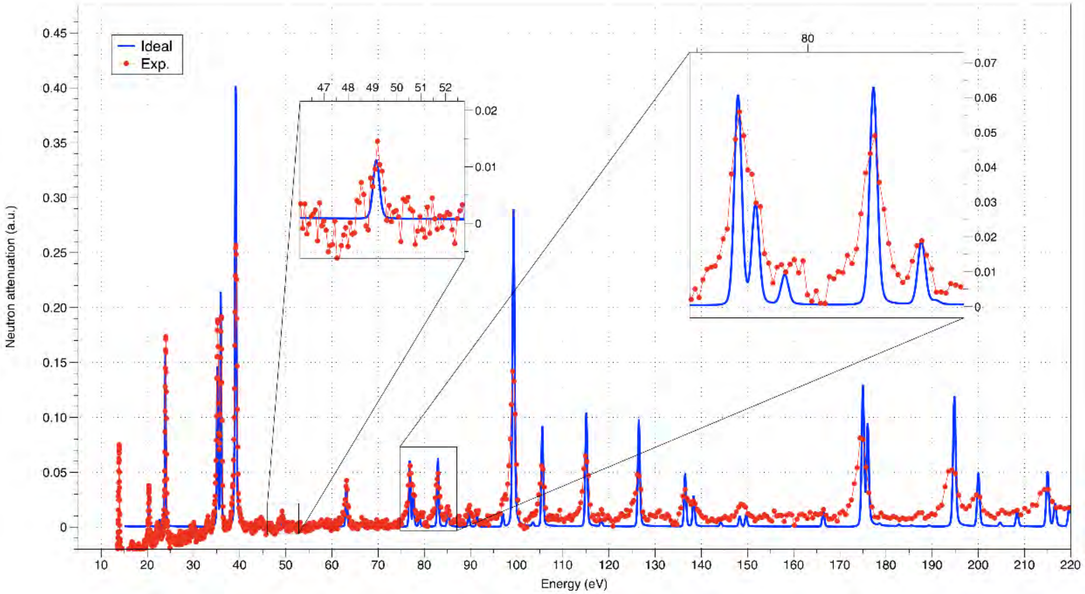

2D resonance imaging measurement of tantalum foil during testing of the lead shielding. The blue data points are the calculated ideal spectrum and the red show the measured spectrum.

- ✓ Measurements performed at SNS with the micro-channel plate (MCP) detector.
- ✓ Technique works great up to neutron energies of ~ 300 eV (heavier elements).
- ✓ However, cannot separate peaks from light elements such as C, H, O, and spatial resolution is ~ 150-200 microns (faster neutrons are harder to slow down and detect).

Principle of wavelength-dependent neutron radiography (or Bragg edge imaging)

- Spallation neutron sources discriminate neutron wavelength (or energy) by using the time-of-flight (TOF) technique

$$I(\lambda) = I_0(\lambda) e^{-\mu(\lambda)x} \qquad \mu(\lambda) = \sigma_t(\lambda) \frac{\rho N_A}{M}$$

2.0 cm

One radiograph

White-beam (or reactor-based) neutron radiograph:
sums over all neutron wavelengths

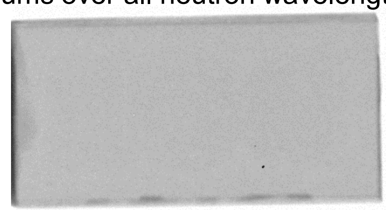

Thousands of radiographs

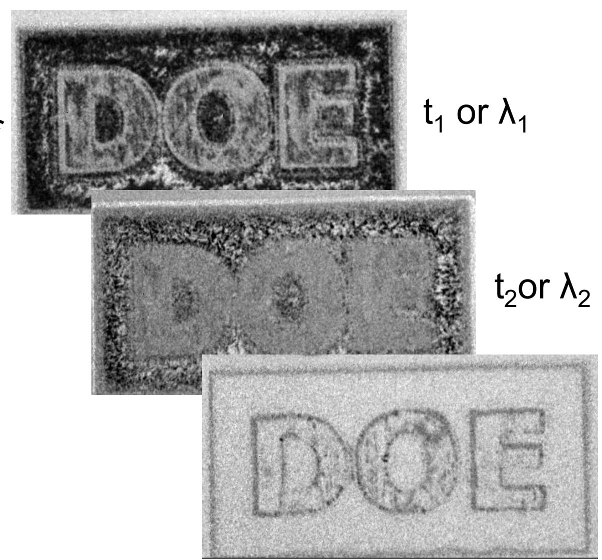

t_1 or λ_1

t_2 or λ_2

t_n or λ_n

Wavelength-dependent (or TOF) neutron radiographs
(**Discrete** neutron wavelengths)

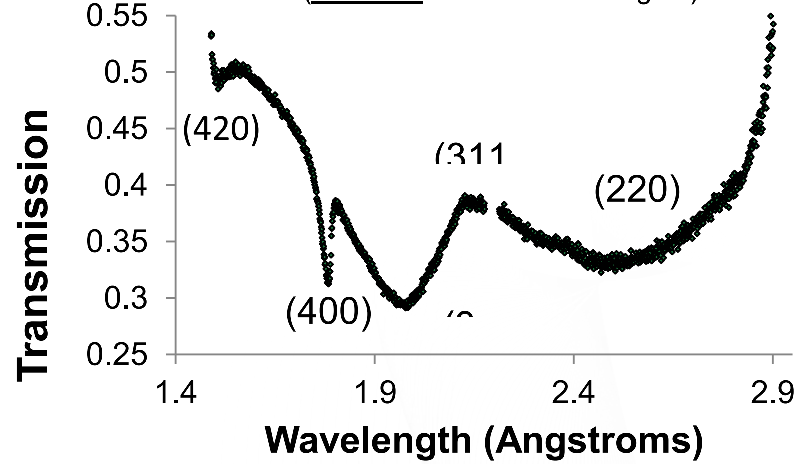


OAK RIDGE NATIONAL LABORATORY'S
MANUFACTURING DEMONSTRATION FACILITY (MDF)
AND
SPALLATION NEUTRON SOURCE

PRESENT

BRAGG EDGE NEUTRON RADIOGRAPHY
OF
INCONEL 718 MADE BY ADDITIVE MANUFACTURING

OAK RIDGE NATIONAL LABORATORY
MANAGED BY UT-BATTELLE FOR THE US DEPARTMENT OF ENERGY

Theory of wavelength-dependent neutron radiography

- $\mathrm{T} = \frac{I(\lambda)}{I_0(\lambda)} = \exp(-n\sigma_{tot}(\lambda)z)$
- $\boxed{\sigma_{tot} = \sigma_{abs} + \sigma_{incoh\ ela} + \sigma_{incoh\ inela} + \sigma_{coh\ inela} + \sigma_{Bragg}}$

Depends on the crystallite size along the beam direction

- $\sigma_{Bragg}(\lambda) = \frac{\lambda^2}{4V_0} \sum_{hkl}^{2d_{hkl}<\lambda} |F_{hkl}|^2 d_{hkl}\, P(\beta_{hkl}) E_{hkl}(\lambda, F_{hkl})$

Most probable angle of preferred grain orientation

- $\beta_{hkl} = \arcsin(\frac{\lambda_{hkl}}{2d_{hkl}})$

Degree of crystalline anisotropy

- $P(\beta_{hkl}) = \frac{1}{\pi}\int_{-\frac{\pi}{2}}^{\frac{\pi}{2}} \left[\left(r_{hkl}^2 - \frac{1}{r_{hkl}}\right)(\cos\alpha_{hkl}(\lambda)\cos\beta_{hkl} - \sin\alpha_{hkl}(\lambda)\sin\beta_{hkl}\sin\varphi)^2 + \frac{1}{r_{hkl}}\right]^{-\frac{3}{2}} d\varphi$, where $\alpha_{hkl} = \left(\frac{\pi}{2}\right) - \arcsin(\frac{\lambda_{hkl}}{2d_{hkl}})$

E. Fermi, W. Sturm, R. Sachs. The transmission of slow neutrons through microcrystalline materials, Physical Review 71 (1947) 589.

Theory of wavelength-dependent neutron radiography (cont'd)

Back-scatter and Laue (forward-scatter) contributions

- $E_{hkl}(\lambda, F_{hkl}) = E_B sin^2\theta_{hkl} + E_L cos^2\theta_{hkl}$
- $E_B = \frac{1}{\sqrt{1+x}}$
- $E_L = 1 - \frac{x}{2} + \frac{x^2}{4} - \frac{5x^3}{48} + \frac{7x^4}{192}$ for x ≤ 1
- $E_L = \sqrt{\frac{2}{\pi x}}\left[1 - \frac{1}{8x} - \frac{3}{128x^2} - \frac{15}{1024x^3}\right]$ for x > 1
- $x = S^2 (\frac{\lambda F_{hkl}}{V_0})^2$, where S is proportional to the crystallite size along the beam direction

T.M. Sabine, R.B. Von Dreele, J.-E. Jorgensen. Extinction in time-of-flight neutron powder diffractometry, Acta Crystallographica Section A 44 (1988) 374-379.
T. Sabine. A reconciliation of extinction theories, Acta Crystallographica Section A: Foundations of Crystallography 44 (1988) 368-374.

Theory of wavelength-dependent neutron radiography (cont'd)

Total cross section for Inconel 718

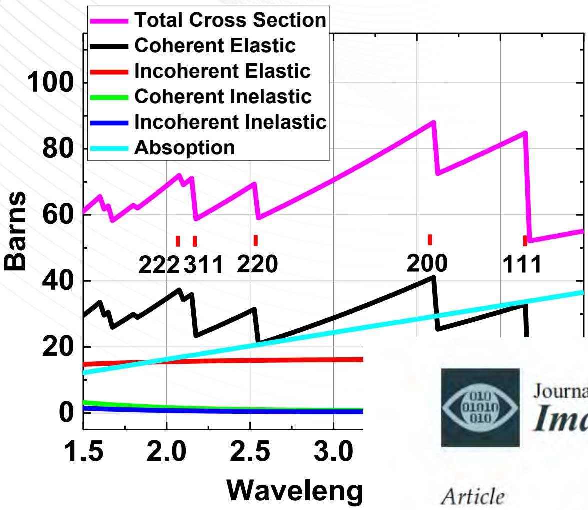

Crystallite size effect (E_{hkl})

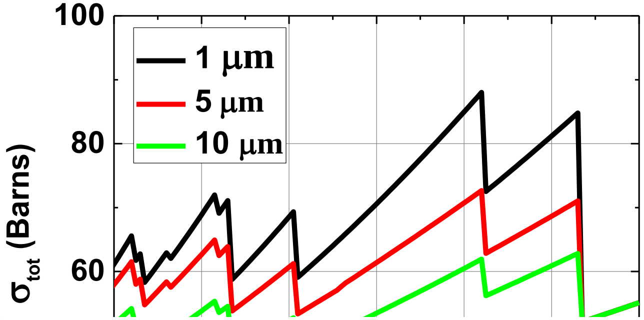

Crystallite orientation effect ($P\left(\alpha_{\vec{h}}(\lambda)\right)$: r and β)

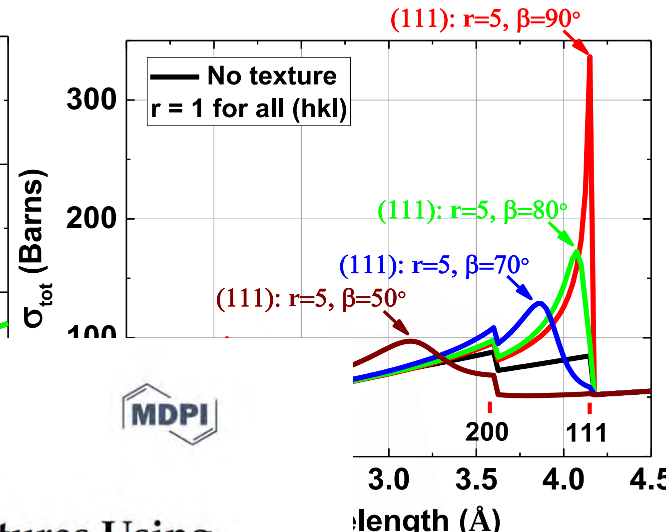

1. Granada, J. R. Zeitschrif
2. 2. Binder, K. physica sta

σ_{Br}

Song, et al., "Ther
Manufactured Met

lelength
of unit cell
or including Debye-
factor
e spacing

s Universität Kiel,

n A. 44, 368-374

Journal of *Imaging*

MDPI

Article

Characterization of Crystallographic Structures Using Bragg-Edge Neutron Imaging at the Spallation Neutron Source †

Gian Song [1,*], Jiao Y. Y. Lin [1], Jean C. Bilheux [1], Qingge Xie [1], Louis J. Santodonato [1], Jamie J. Molaison [1], Harley D. Skorpenske [1], Antonio M. Dos Santos [1], Chris A. Tulk [1], Ke An [1], Alexandru D. Stoica [1], Michael M. Kirka [2], Ryan R. Dehoff [2], Anton S. Tremsin [3], Jeffrey Bunn [1], Lindsay M. Sochalski-Kolbus [1] and Hassina Z. Bilheux [1,*]

1 Neutron Scattering Division, Neutron Sciences Directorate, Oak Ridge National Laboratory, Oak Ridge, TN 37830, USA; linjiao@ornl.gov (J.Y.Y.L.); bilheuxjm@ornl.gov (J.C.B.); xieq@ornl.gov (Q.X.); santodonatol@ornl.gov (L.J.S.); molaisonjj@ornl.gov (J.J.M.); skorpenskehd@ornl.gov (H.D.S.); dossantosam@ornl.gov (A.M.D.S.); tulkca@ornl.gov (C.A.T.); kean@ornl.gov (K.A.); stoicaad@ornl.gov (A.D.S.); bunnjr@ornl.gov (J.B.); Lindsay.sochalski@gmail.com (L.M.S.-K.)

OAK RIDGE National Laboratory

Validation of Bragg-edge imaging results using neutron diffraction

Bragg edge CT at SNS SNAP

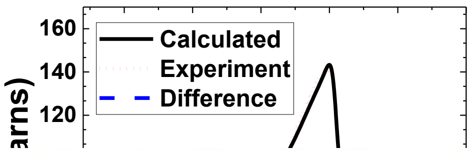

Texture measurements at SNS VULCAN

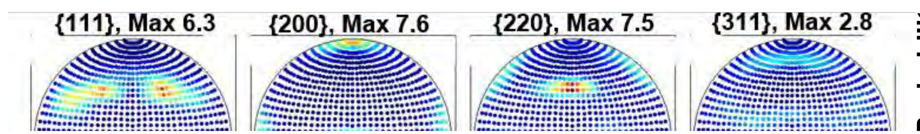

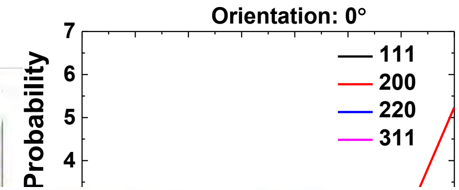

Applying neutron transmission physics and 3D statistical full-field model to understand 2D Bragg-edge imaging

Q. Xie,[1,a)] G. Song,[1,a)] S. Gorti,[2] A. D. Stoica,[1] B. Radhakrishnan,[2] J. C. Bilheux,[1] M. Kirka,[3] R. Dehoff,[3] H. Z. Bilheux,[1,b)] and K. An[1,b)]

[1]*Neutron Scattering Division, Oak Ridge National Laboratory, Oak Ridge, Tennessee 37831, USA*

[2]*Computational Sciences and Engineering Division, Oak Ridge National Laboratory, Oak Ridge, Tennessee 37831, USA*

[3]*Materials Science and Technology Division, Oak Ridge National Laboratory, Oak Ridge, Tennessee 37831, USA*

(Received 14 November 2017; accepted 22 January 2018; published online 15 February 2018)

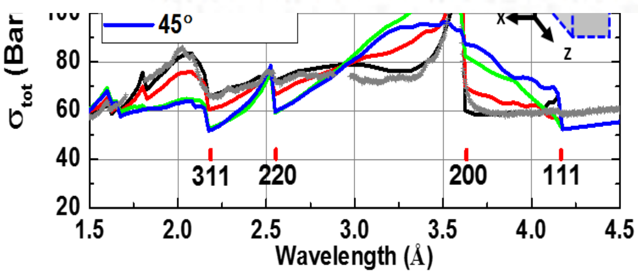

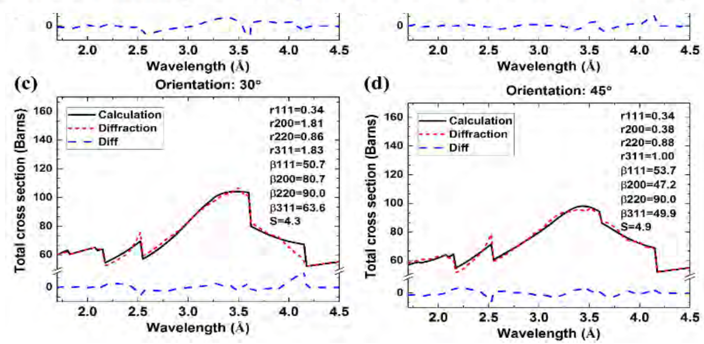

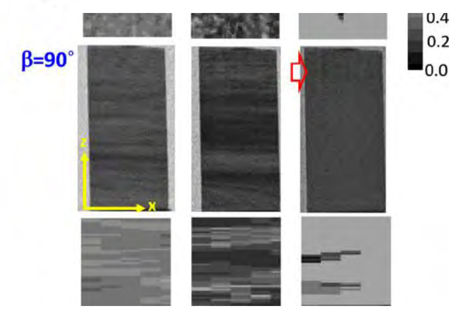

SNS SNAP Imaging (“Temporary” Capability n user program)

Game #2: What is this peak due to?

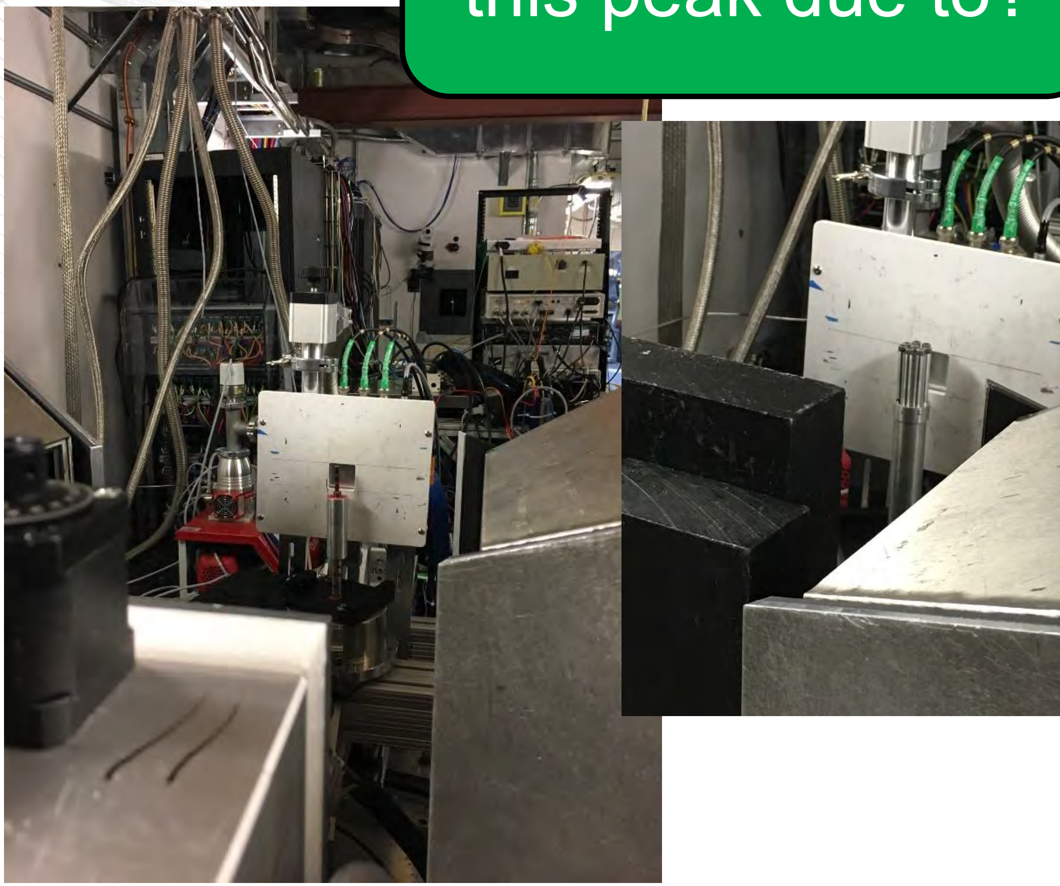

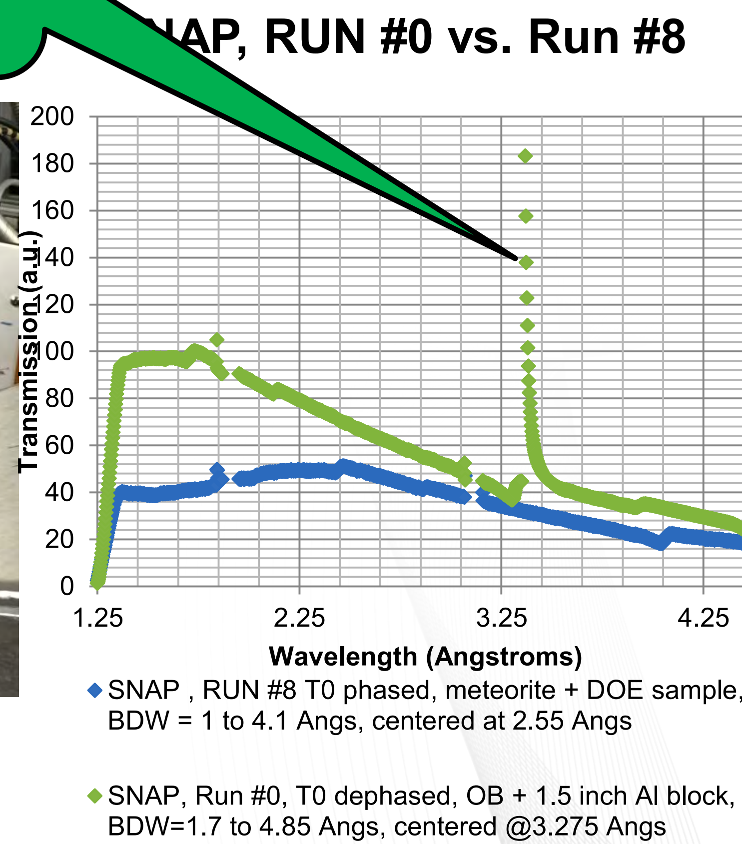

Neutron radiography and data reduction at a pulsed source

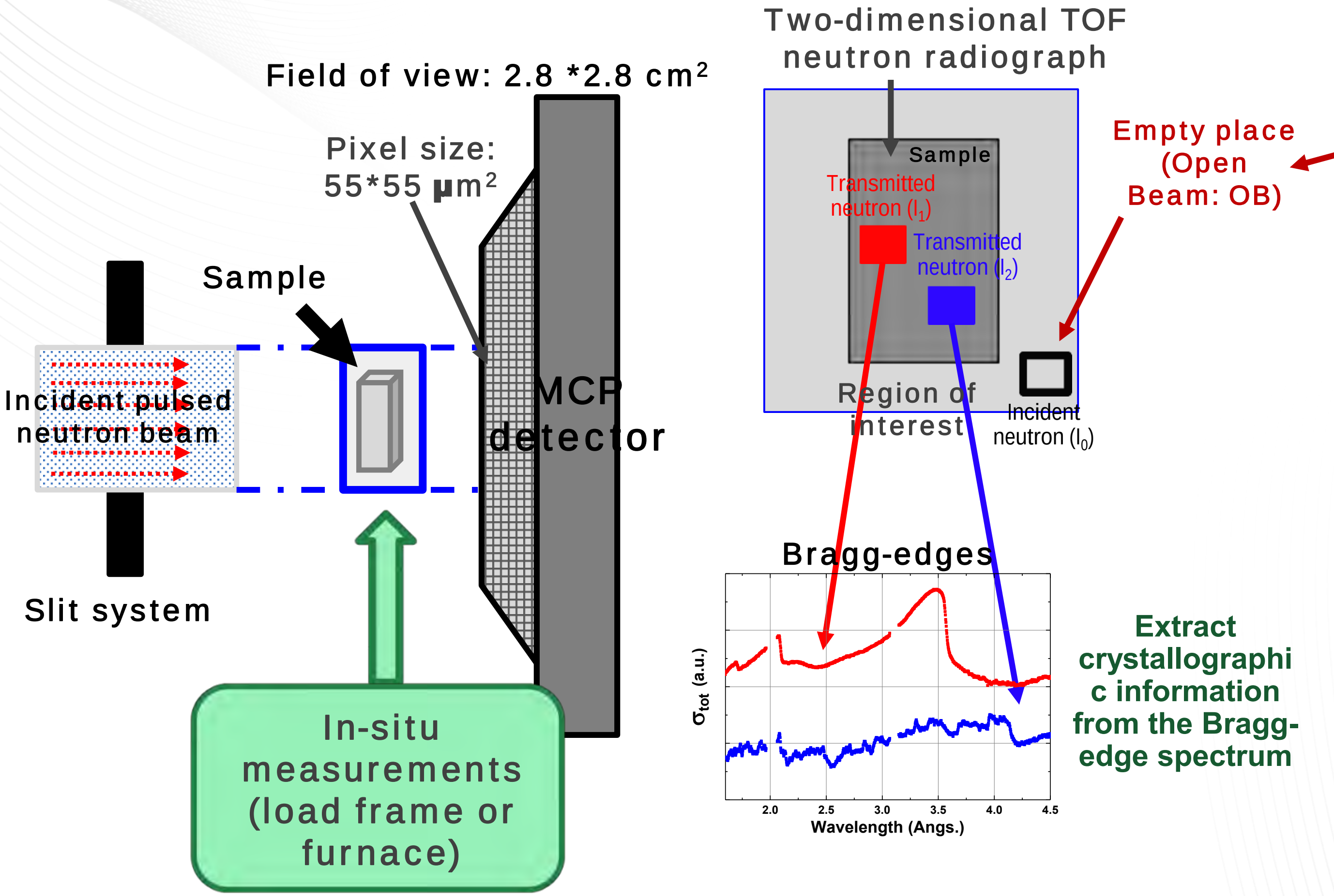

Best option for data reduction but sometimes sample occupies whole detector area

Second best option is to use a beam monitor

SNS energy distribution varies as a function of beam power

Cannot measure as a function of time but need to measure as a function of protons on target

Gamma discrimination is extremely important for resonance imaging

Engineering Materials

Many samples prepared using two Inconel 718 blocks with different crystallite structures

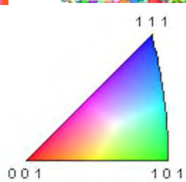

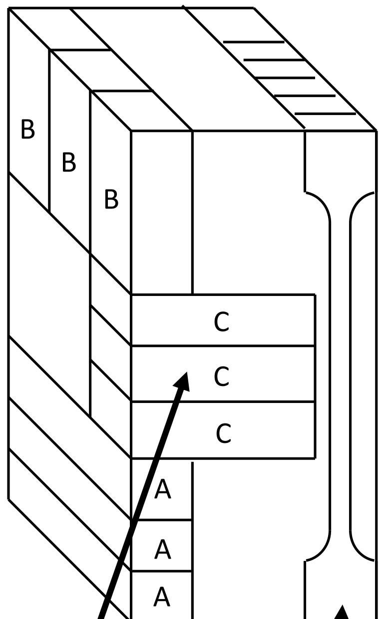

NECCESSARILY TO SCALE; FOR ILLUSTRATIV

Compression samples
(~ 12 x 5 x 5 mm^3)

Tensile samples
(~ 30 x 5 x 5 mm^3)

Oak Ridge National Laboratory

In-situ heating of AM Columnar Inconel 718 coupon

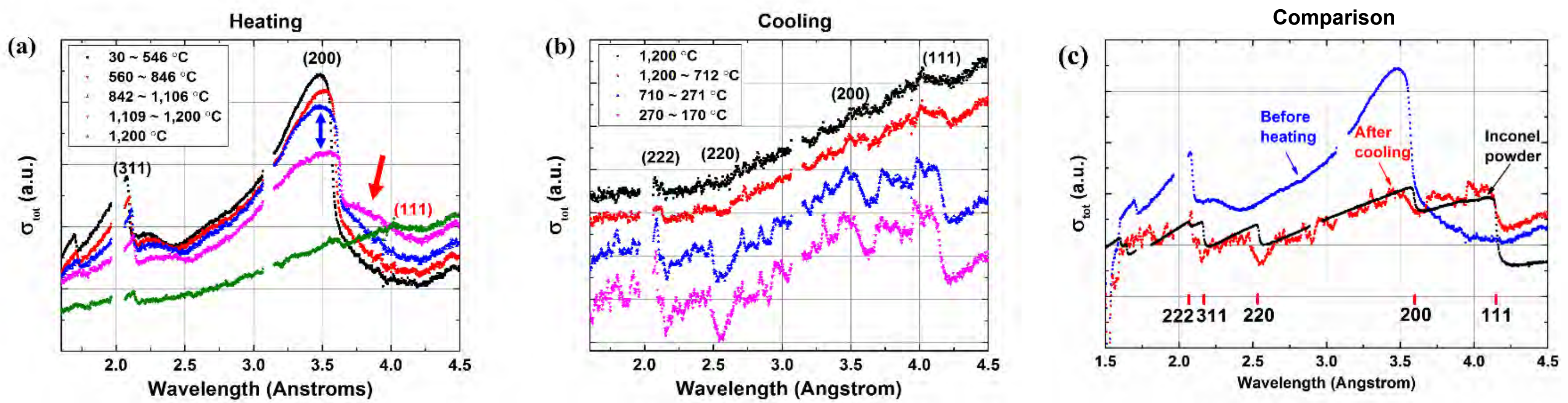

- Before heating: two dominant microstructure orientations (200) and (311)
- As temperature increases, Bragg edge shifts toward higher λ, as expected during thermal expansion
- Bragg edges decrease with increased temperature due to Debye Waller effect (grain vibrations)
- During cooling, decrease of (200) and presence of (111) grains
- Final microstructure close to powder sample data (i.e. random grain orientation)
- Data arbitrarily shifted along y-axis to show the different plots

Fitting and interpretation of the data

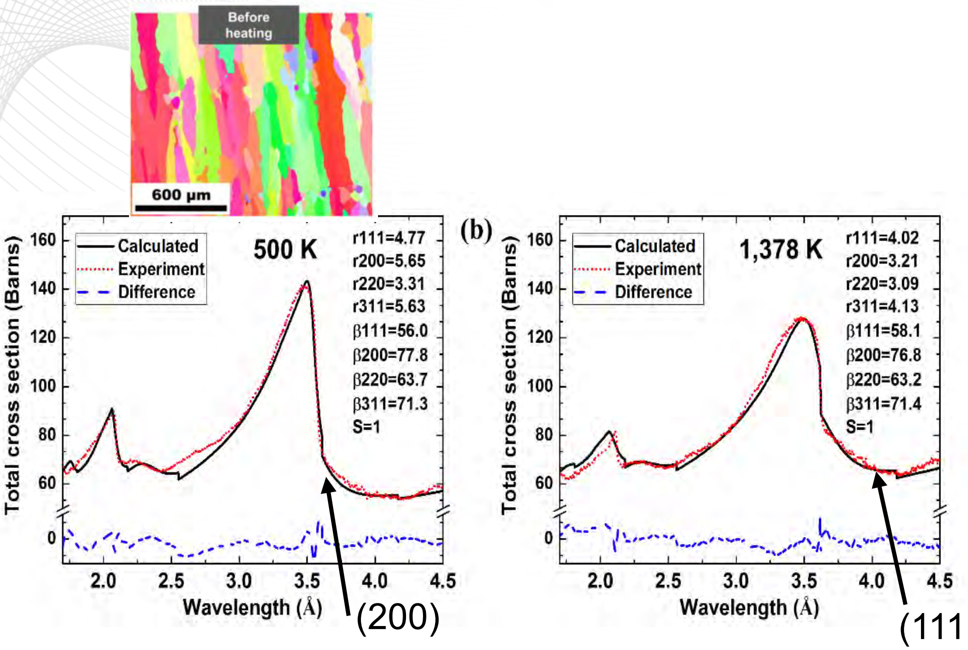

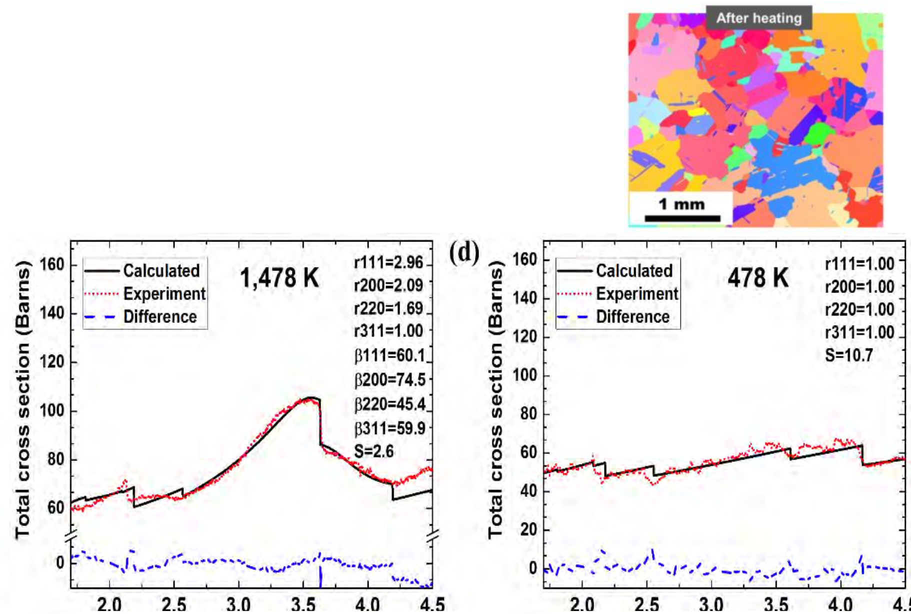

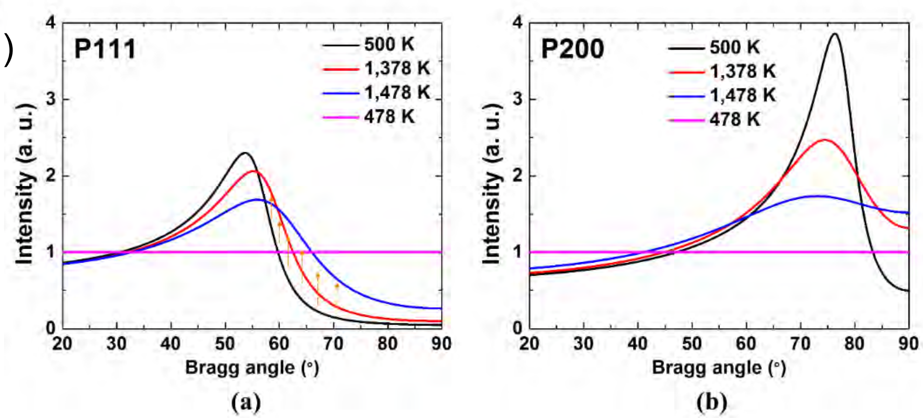

- r_{hkl} = 1, random grain orientation
- r_{hkl} =/ 1, fiber or plate-shaped distribution (i.e. here columnar)
- S (in microns) increases as a function of temperature, from 1 to 2.6, and finally reaching 10.7, indicating grain size growth

Bragg edge fitting with Jupyter Notebooks

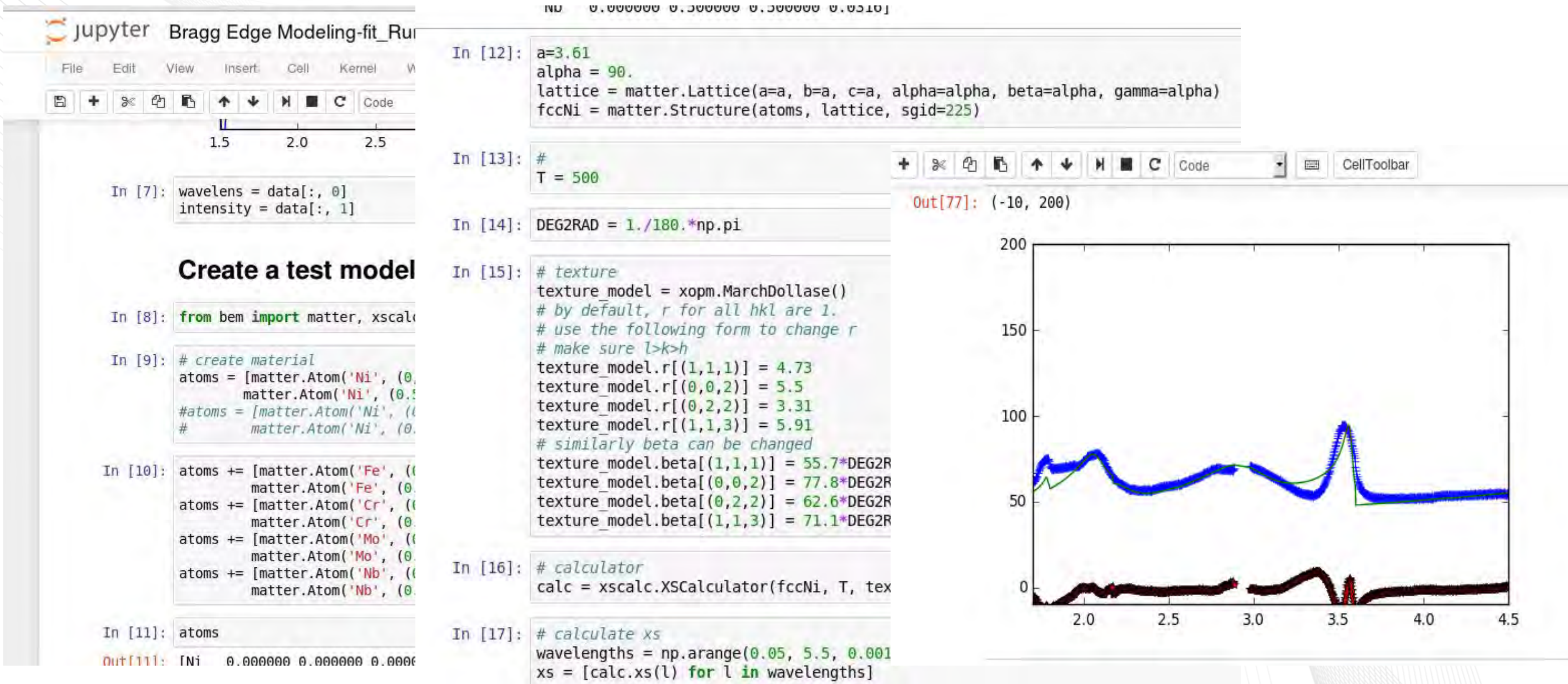

OAK RIDGE
National Laboratory

Software: a required tool for accurate and fast processing of wavelength-dependent neutron radiography: iBeatles

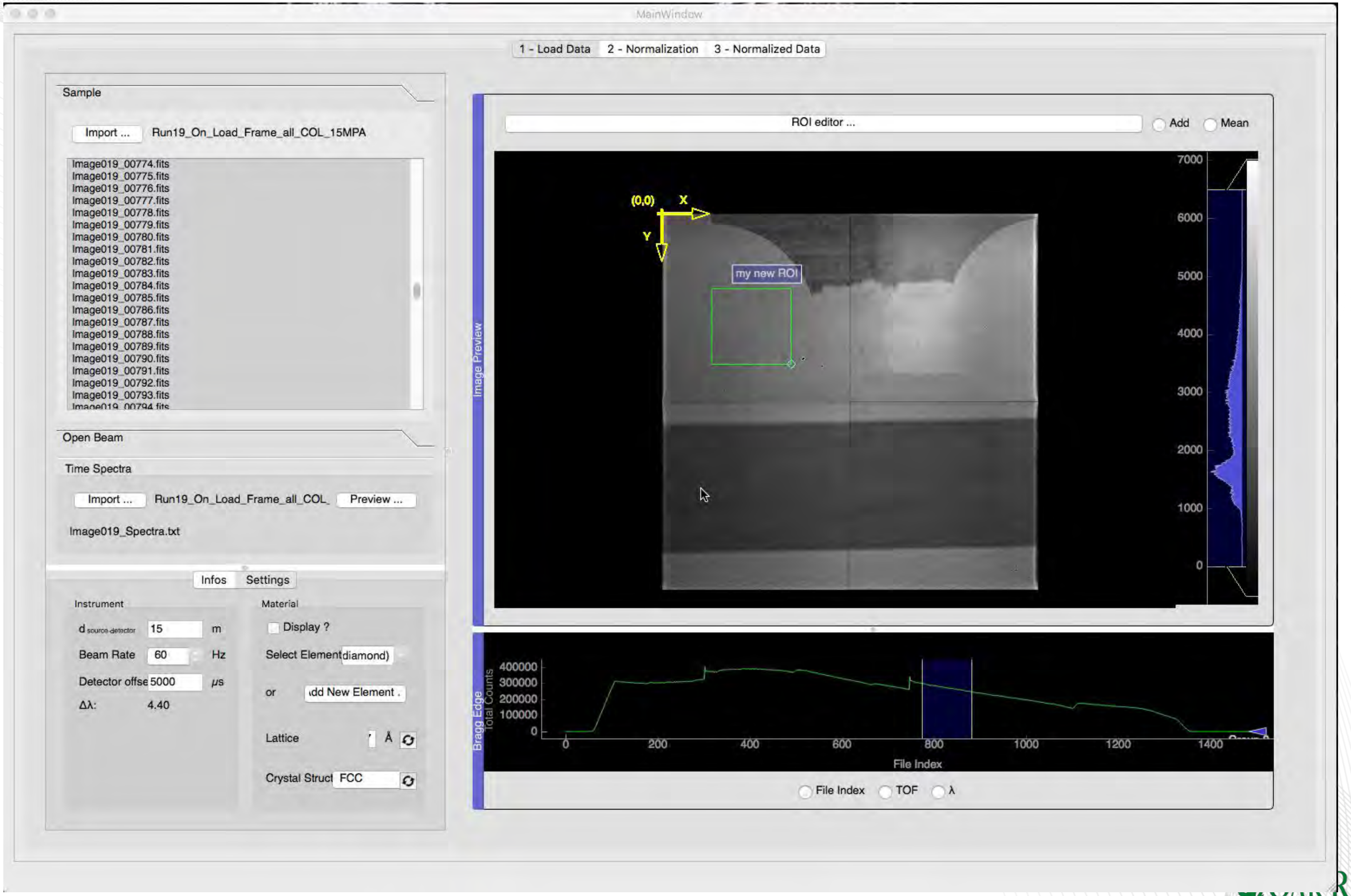

OAK RIDGE National Laboratory

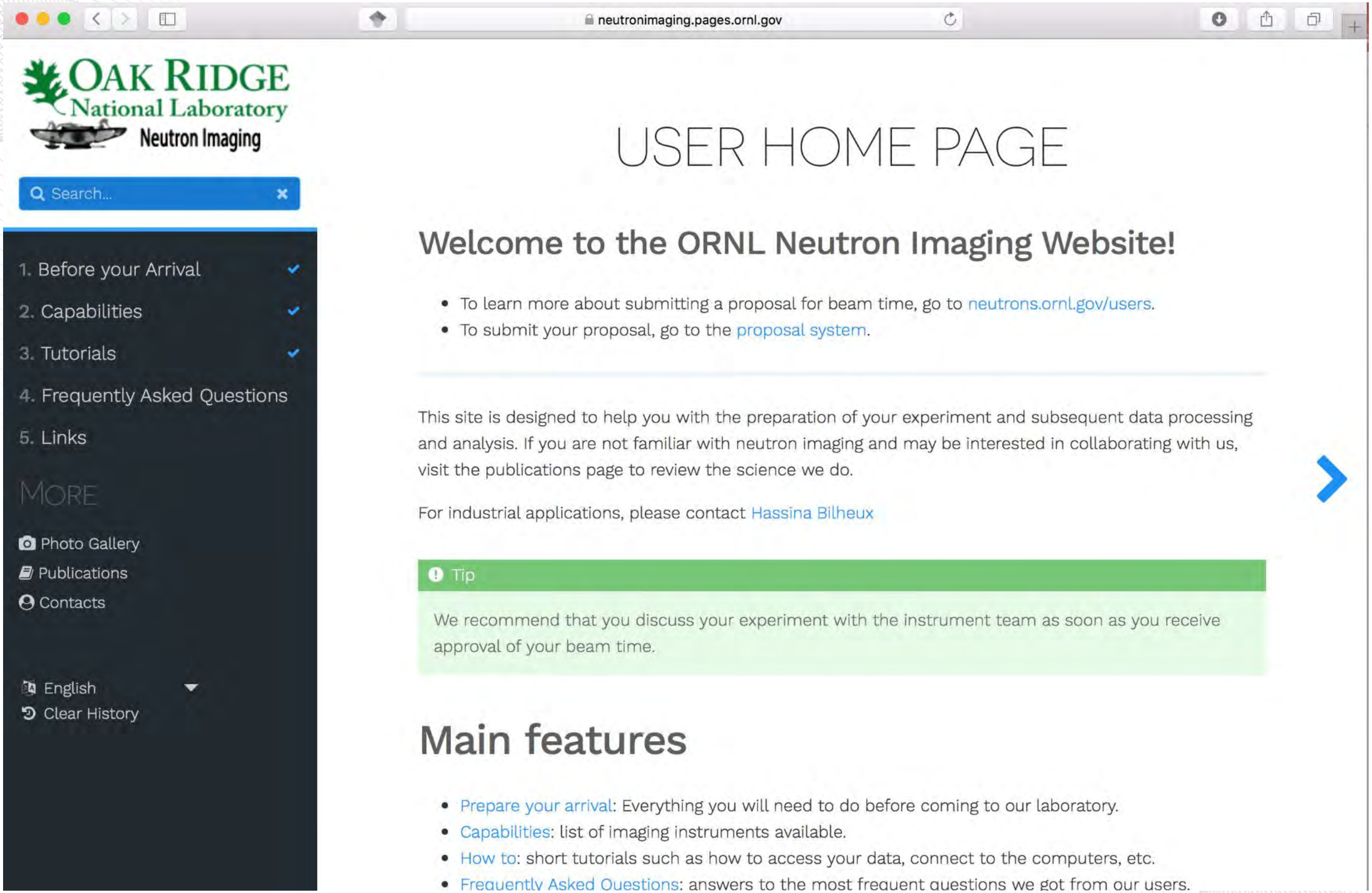
neutronimaging.pages.ornl.gov
OAK RIDGE National Laboratory
Neutron Imaging
Search...
1. Before your Arrival
2. Capabilities
3. Tutorials
4. Frequently Asked Questions
5. Links
MORE
Photo Gallery
Publications
Contacts
English
Clear History
USER HOME PAGE
Welcome to the ORNL Neutron Imaging Website!
To learn more about submitting a proposal for beam time, go to neutrons.ornl.gov/users.
To submit your proposal, go to the proposal system.
This site is designed to help you with the preparation of your experiment and subsequent data processing and analysis. If you are not familiar with neutron imaging and may be interested in collaborating with us, visit the publications page to review the science we do.
For industrial applications, please contact Hassina Bilheux
Tip
We recommend that you discuss your experiment with the instrument team as soon as you receive approval of your beam time.
Main features
Prepare your arrival: Everything you will need to do before coming to our laboratory.
Capabilities: list of imaging instruments available.
How to: short tutorials such as how to access your data, connect to the computers, etc.
Frequently Asked Questions: answers to the most frequent questions we got from our users.

neutronimaging.pages.ornl.gov

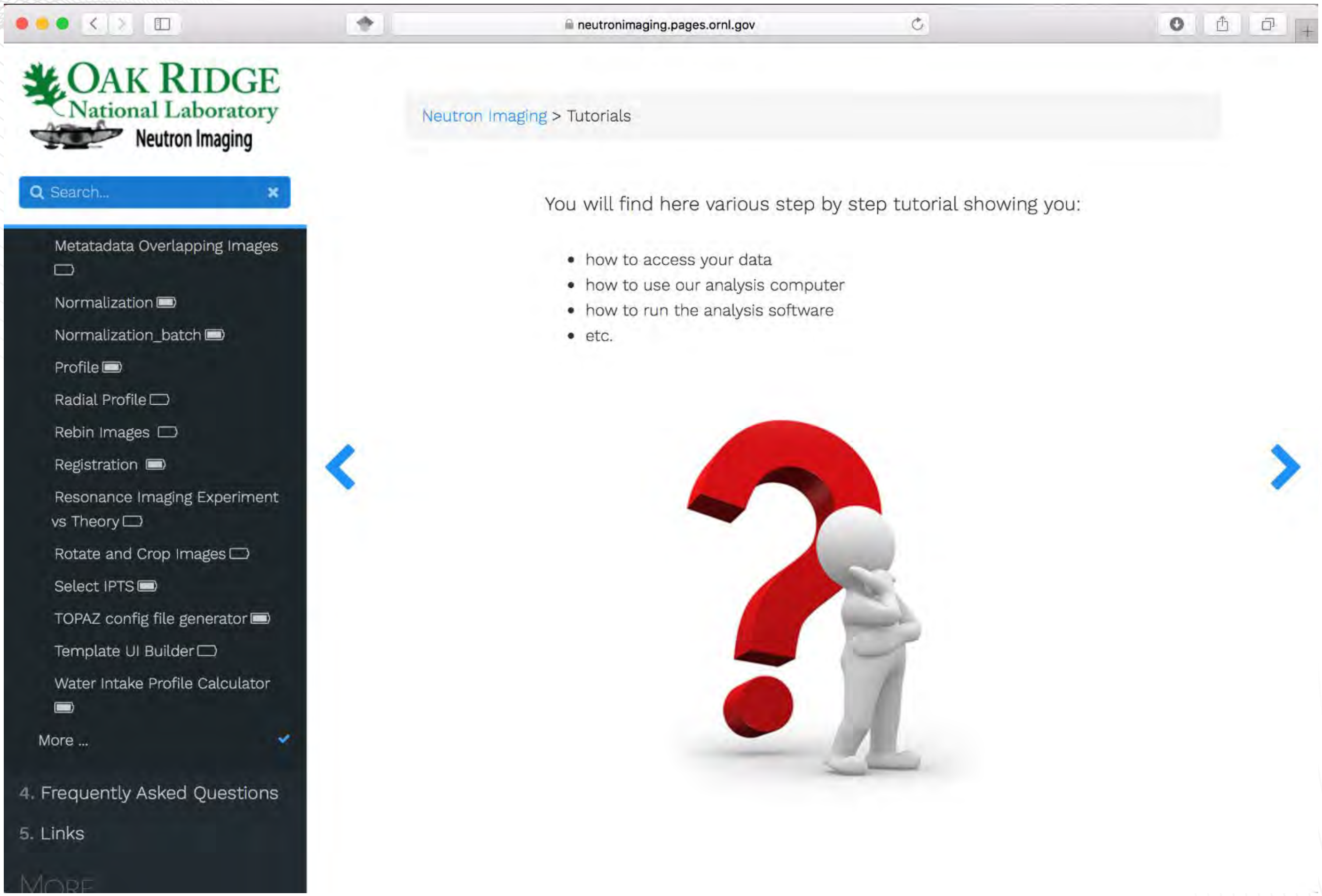

Step-by-step tutorials with animated demonstrations

Something you want to see on our user website? Contact Jean Bilheux bilheuxjm@ornl.gov

Image Processing and Analysis

- Data normalization and 3D reconstruction are considered part of the pre-processing steps
- Image Processing and Analysis are often complex when trying to quantify data and require three main ingredients:
  - advanced skills
  - “good” size computer/server
  - advanced visualization techniques/software to interact with your data
- We don’t expect you to know how to do this, but we expect you to help us develop the algorithms to extract the information you need
  - Not just “pretty pictures” but a 3D quantitative technique

Fabrication tolerance studies comparing CAD drawing to neutron computed tomography

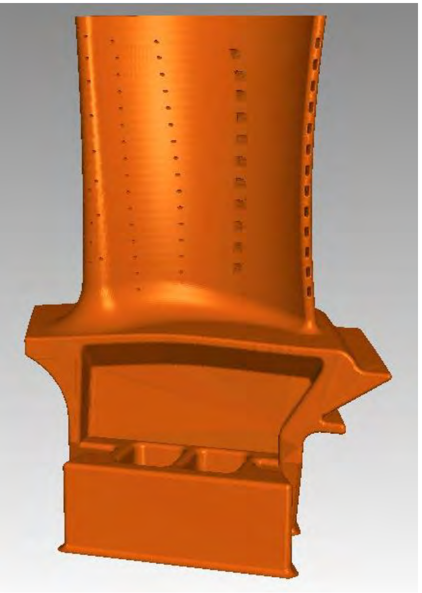

Engineering drawing

+

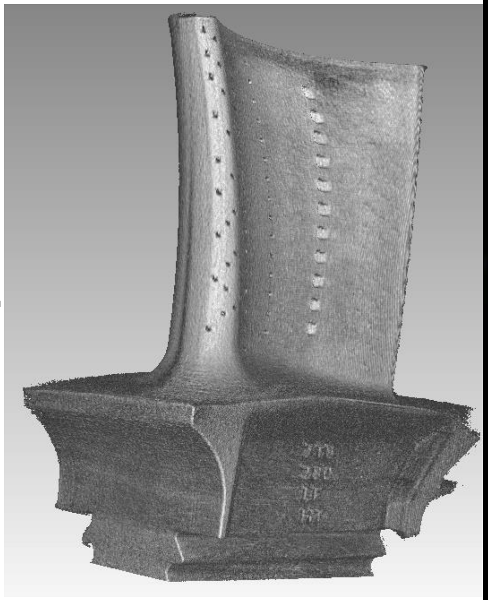

Neutron CT

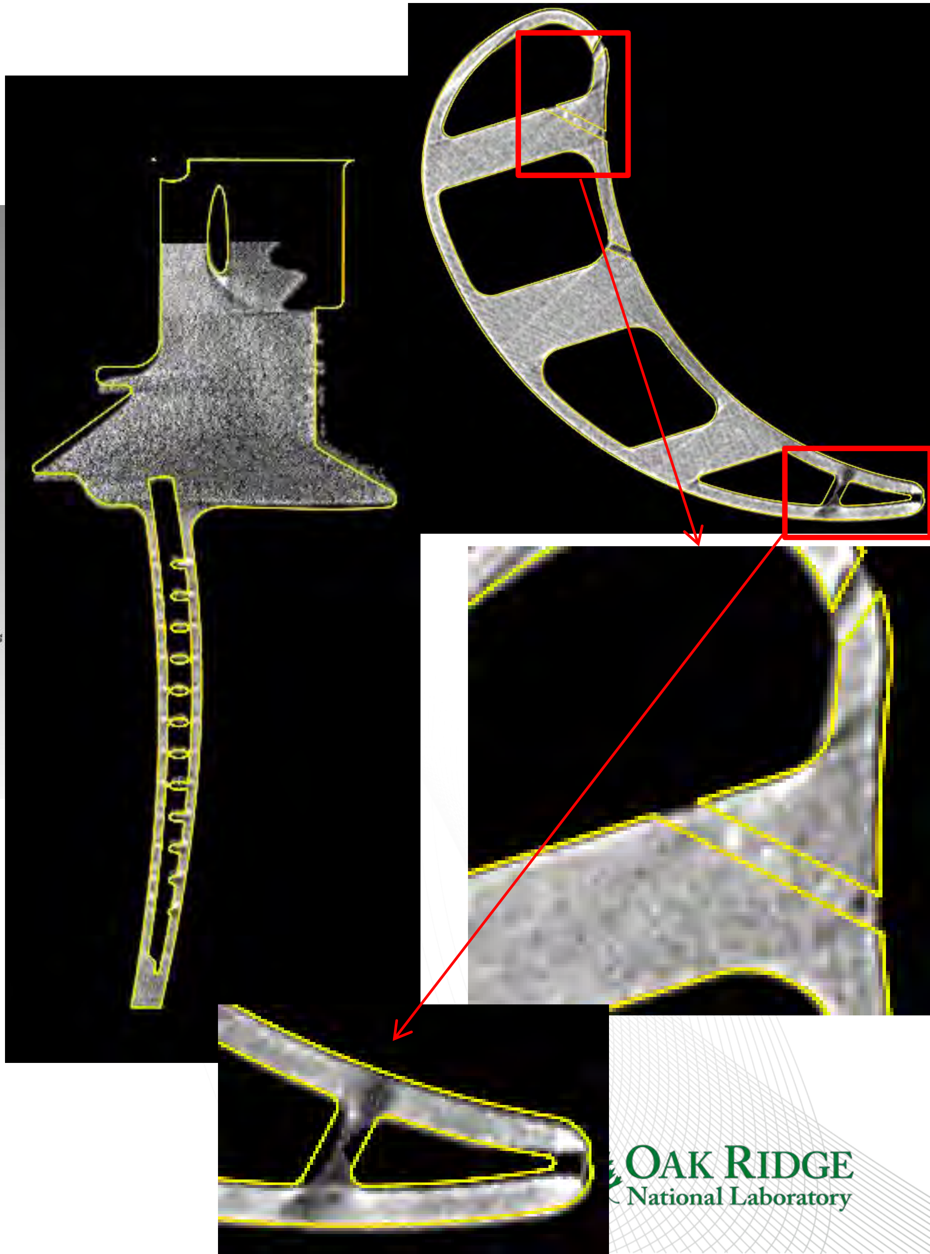

In orange/yellow: AUTOCAD outline
In gray: neutron data


The Oak Ridge National Laboratory
Manufacturing Demonstration Facility
&
High Flux Isotope Reactor
Present
Neutron Computed Tomography of an
Inconel 718 Turbine blade made by
Additive Manufacturing
OAK RIDGE
National Laboratory

Micro X-ray CT of AM samples

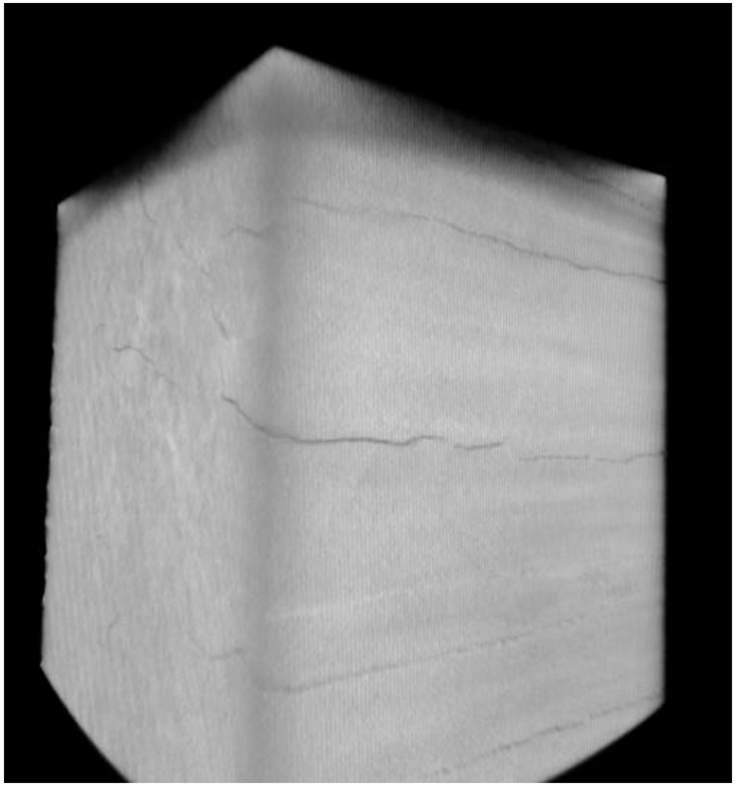

5 mm x 5 mm base Inconel 718

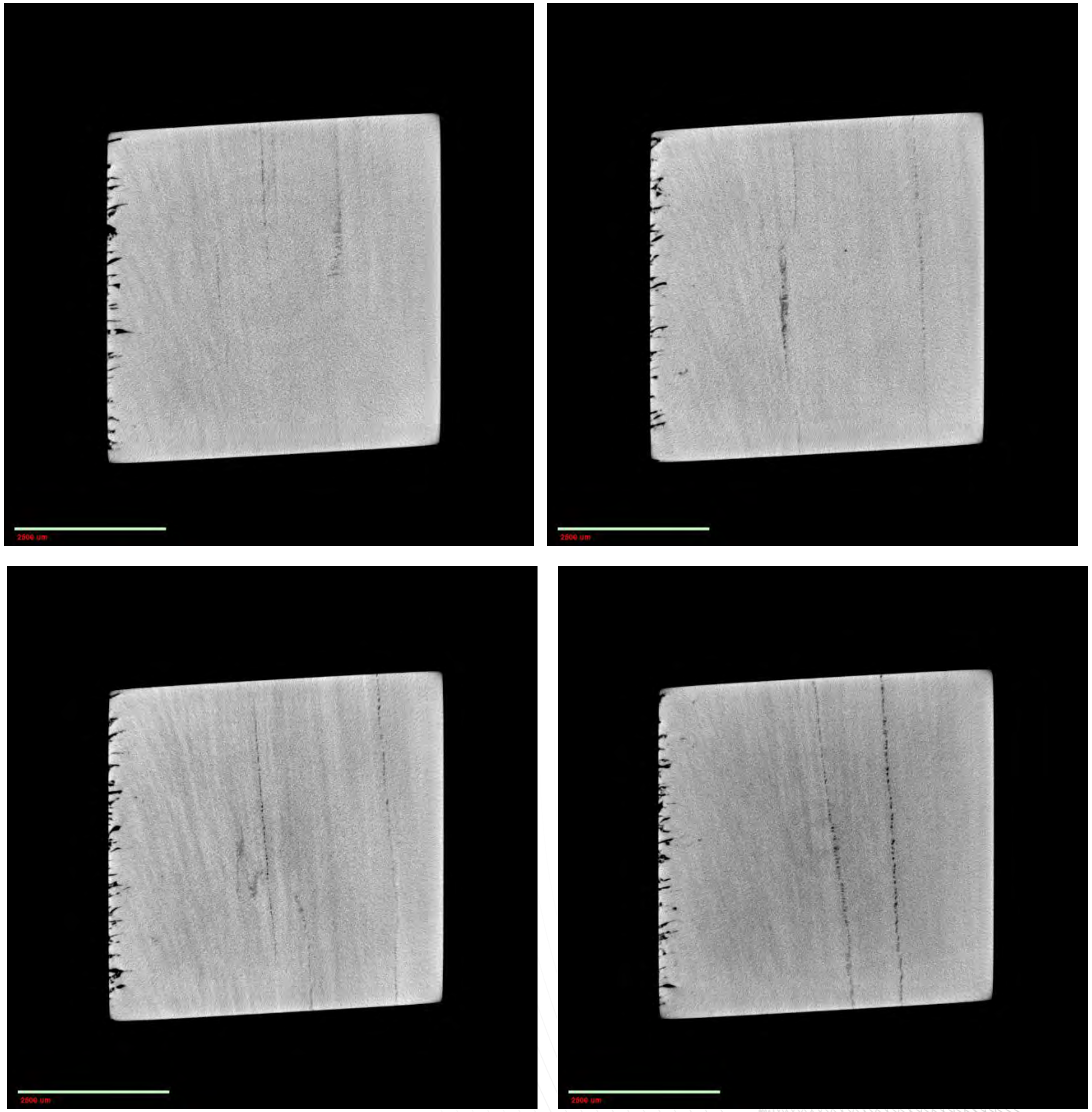

OAK RIDGE National Laboratory

The Nature of Electrochemical Delithiation of Li-Mg Alloy Electrodes: Neutron Computed Tomography and Analytical Modeling

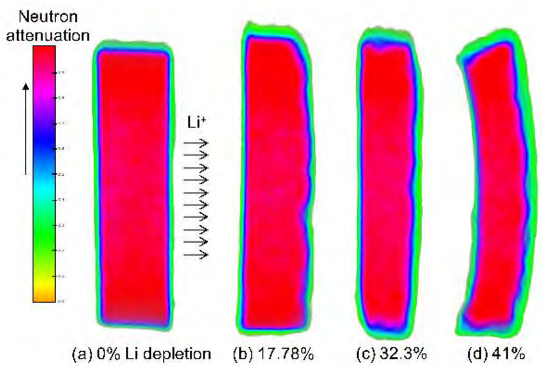

Top: Cross-sectional views of 3D reconstructed pseudo-color images of Mg-70 wt.% (~89 at.%) Li alloy depleted to various depths.
Bottom: Simulated vs. experimental data for Mg-70 wt.% Li with depletion of (a) 0%, (b) 17.78%, (c) 32.34% and (d) 41%.

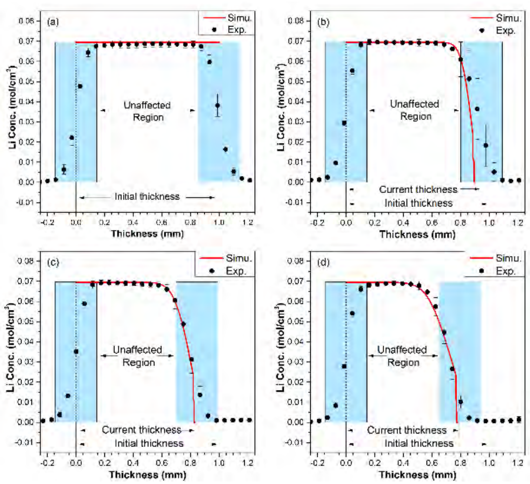

Y. Zhang, K.S.R. Chandran, M. Jagannathan, H.Z. Bilheux, J.C. Bilheux, Journal of The Electrochemical Society, 164 (2017) A28-A38.

Scientific Achievement

Li concentration profiles in electrochemically delithiated Li-Mg alloy electrodes have been quantitatively determined using neutron computed tomography (CT). A rigorous analytical model to quantify the diffusion-controlled delithiation, accompanied by phase transition and phase boundary movement, has also been developed.

Significance and Impact

- The variations in Li conc. caused by different depths of delithiation can be clearly observed in the neutron tomographic data.
- The simulated Li concentration profiles agreed well with the tomographic data. The modeling approach is exact and is applicable for modeling delithiation of any Li-containing electrode.
- Neutron CT can be used to validate kinetic model for Li-containing electrode.

Research Details

- Alloy electrodes with two compositions, Mg-70 wt.% Li and Mg-50 wt.% Li, were delithiated to various depths of Li depletion in Swagelok cells.
- Neutron CT scan was performed at CG-1D beamline using a charge-coupled device (CCD).
- Analytical solutions for Li conc. profile were obtained by solving Fick's second law using variable separation method with initial and boundary conditions.
- Li diffusivity used for modeling was validated by chronoamperometric test and Cottrell equation.

This research was supported by DoE-BES grant DE-FG0212ER46891. Measurement was performed at the ORNL High Flux Isotope Reactor CG-1D imaging beamline. This effort was supported by Scientific User Facilities Division, Office of Basic Energy Sciences, US Department of Energy.

OAK RIDGE National Laboratory

Neutron Radiography and CT of batteries

- **Can spatially map inhomogeneities and degradation of the cell in 2D (in-operando) and 3D (ex-situ)**
- **Quantitative measure of Li concentration: correlates contrast with local Li concentration**

2D

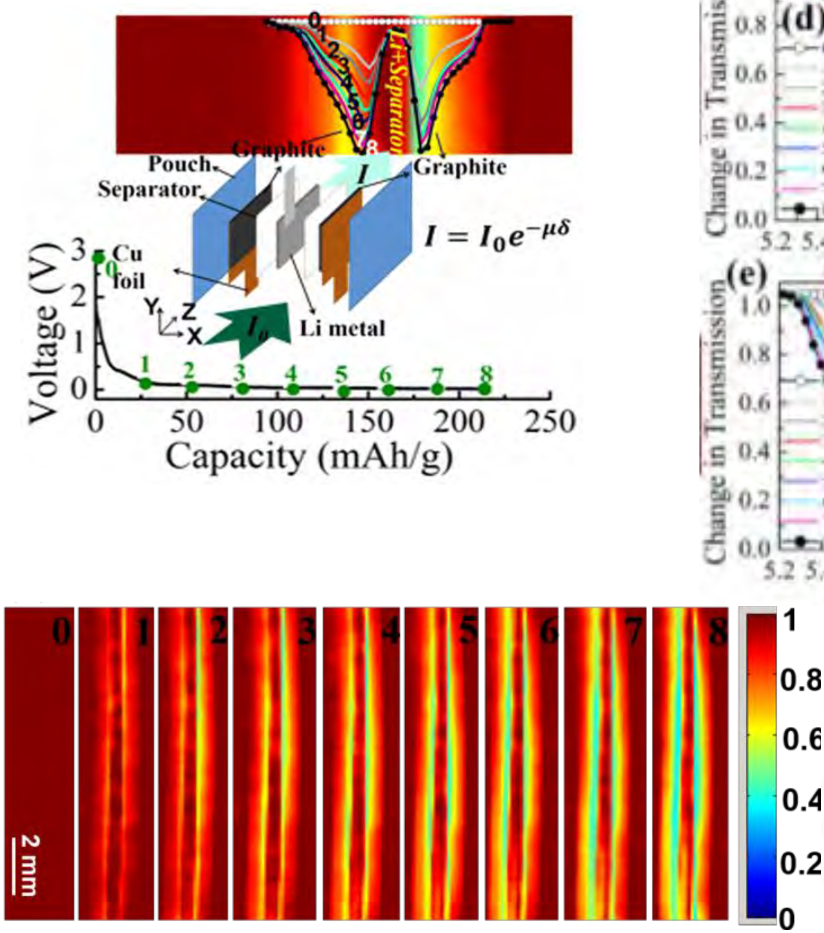

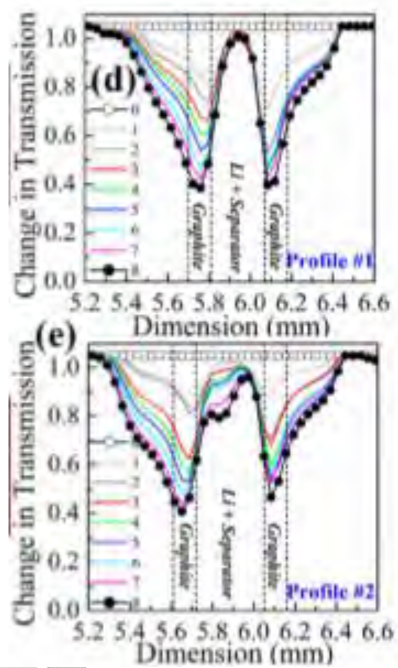

3D

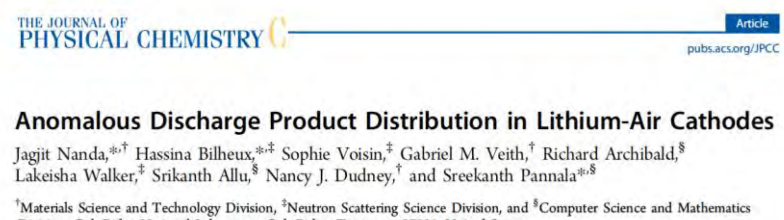
THE JOURNAL OF PHYSICAL CHEMISTRY C

Article

pubs.acs.org/JPCC

Anomalous Discharge Product Distribution in Lithium-Air Cathodes

Jagjit Nanda,*,† Hassina Bilheux,*,‡ Sophie Voisin,‡ Gabriel M. Veith,† Richard Archibald,§ Lakeisha Walker,‡ Srikanth Allu,§ Nancy J. Dudney,† and Sreekanth Pannala*,§

†Materials Science and Technology Division, ‡Neutron Scattering Science Division, and §Computer Science and Mathematics Division, Oak Ridge National Laboratory, Oak Ridge, Tennessee 37831, United States

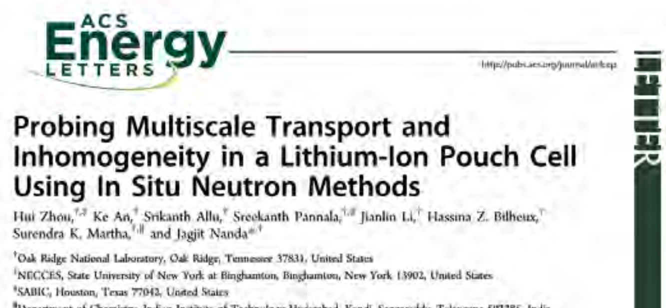
ACS Energy LETTERS

Probing Multiscale Transport and Inhomogeneity in a Lithium-Ion Pouch Cell Using In Situ Neutron Methods

Hui Zhou,†,‡ Ke An,† Srikanth Allu,† Sreekanth Pannala,†,‡ Jianlin Li,† Hassina Z. Bilheux,† Surendra K. Martha,†,∥ and Jagjit Nanda*,†

†Oak Ridge National Laboratory, Oak Ridge, Tennessee 37831, United States
‡NECCES, State University of New York at Binghamton, Binghamton, New York 13902, United States
SABIC, Houston, Texas 77042, United States
∥Department of Chemistry, Indian Institute of Technology Hyderabad, Kandi, Sangareddy, Telangana 502285, India

OAK RIDGE National Laboratory

How to enhance contrast in batteries other than Li batteries?

Isotope	Coh xs	Inc xs	Scatt xs	Abs xs
Zn	4.054	0.077	4.131	1.11
64Zn	3.42	0	3.42	0.93
66Zn	4.48	0	4.48	0.62
67Zn	7.18	0.28	7.46	6.8
68Zn	4.57	0	4.57	1.1
70Zn	4.5	0	4.5(1.5)	0.092

- ✓ Technique resolution and contrast, based on fitting amplitude and shift of signal is decoupled from the instrument resolution.
- ✓ Capability to detect features down to 500 nm.

$$n(x,y,z) = 1 - \underbrace{\delta(x,y,z)}_{\text{phase}} + \underbrace{i\beta(x,y,z)}_{\text{attenuation}}$$

$$d = \frac{l^{2} N b_c}{2p} \qquad b = s_t(l)\frac{r N_A}{M}\frac{l}{2p}$$

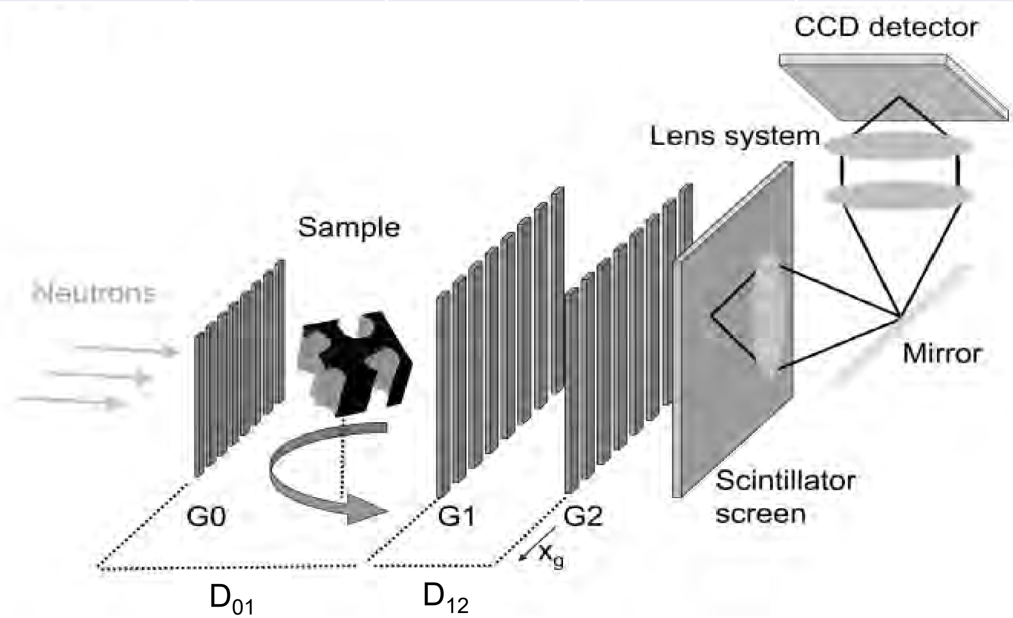

C. Grünzweig, F. Pfeiffer, O. Bunk, T. Donath, G. Kühne, G. Frei, M. Dierolf, C. David, Design, fabrication, and characterization of diffraction gratings for neutron phase contrast imaging. Review of Scientific Instruments 79, - (2008).

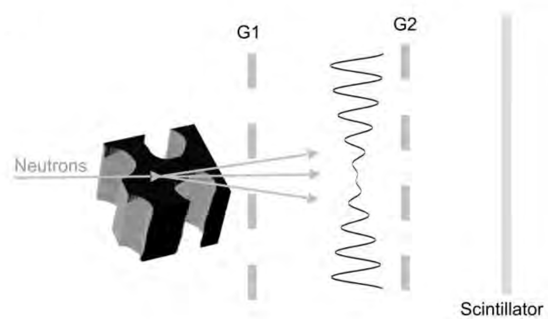

Neutron Grating Interferometry (nGI) at CG-1D

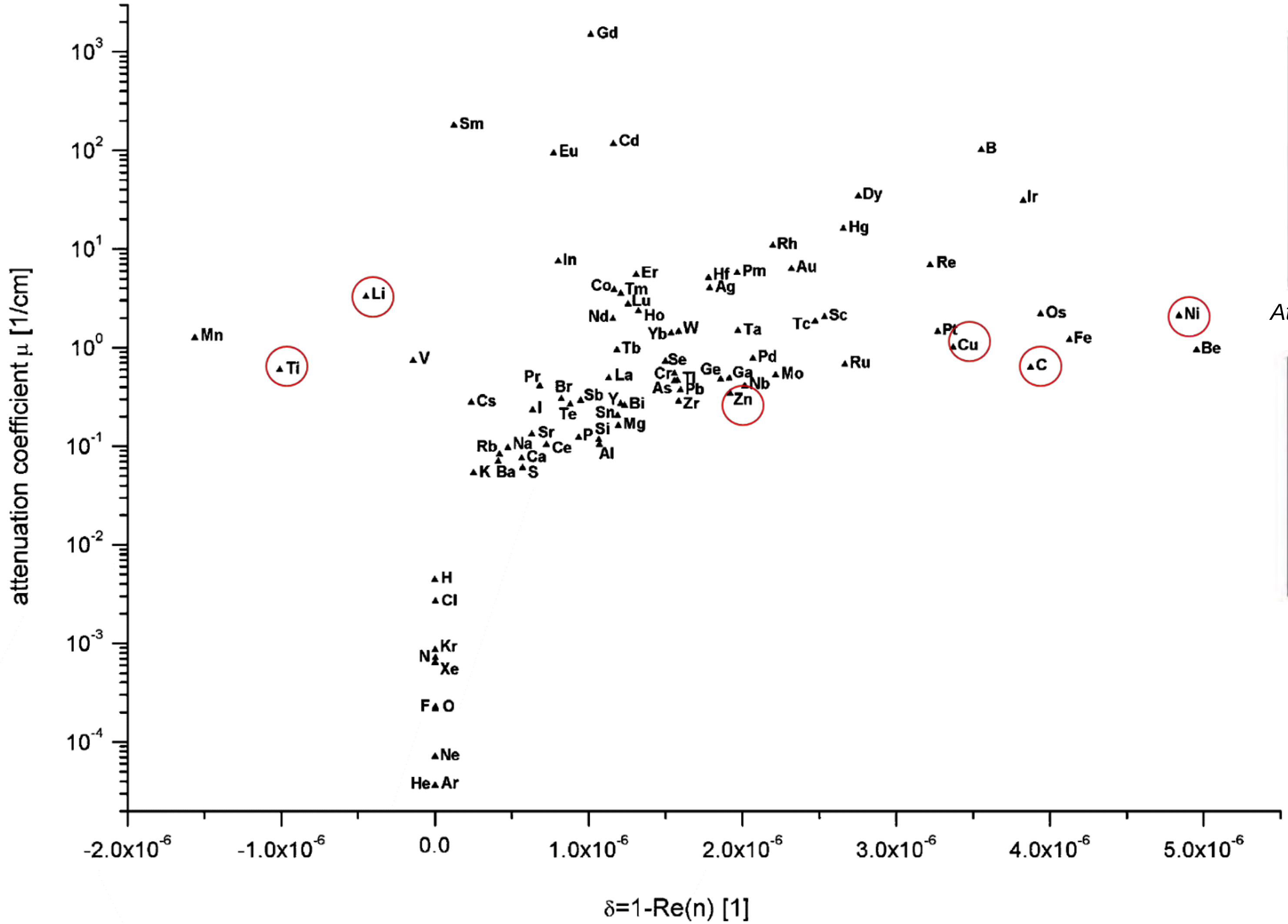

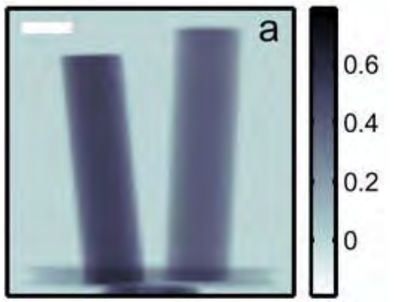

Attenuation-based radiograph of Cu and Ti samples.

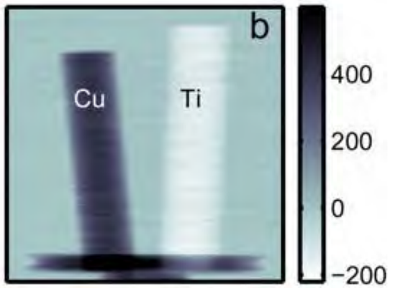

Neutron phase shift values projected on each pixel.

E. Lehmann, K. Lorenz, , E. Steicheleb, P. Vontobel, Non-destructive testing with neutron phase contrast, Nuclear Instruments and Methods A 542, 2005.

Rapid Imbibition of Water in Fractures within Unsaturated Sedimentary Rock

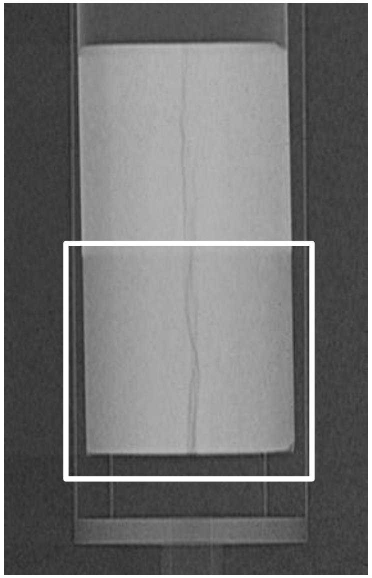

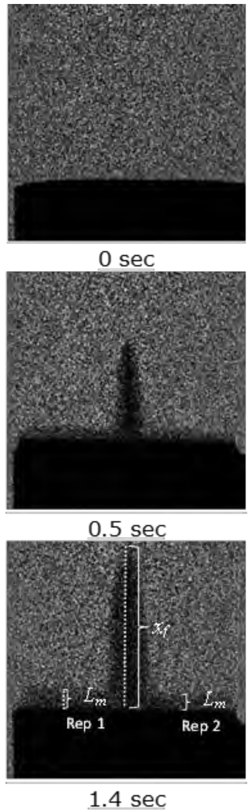

Time sequence of neutron radiographs showing the rapid uptake of water into a longitudinal, air-filled fracture zone in Berea sandstone (~50 mD). FOV is ~28 x 28 mm^2.

Work performed at the High Flux Isotope Reactor Imaging beam line (CG1D) was supported by the Scientific User Facilities Division, Office of Basic Energy Sciences, U.S. Department of Energy.

Scientific Achievement

Spontaneous imbibition of liquids into gas-filled fractures in variably-saturated porous media is important in a variety of engineering and geological contexts. Dynamic neutron radiography was applied to directly quantify this phenomenon in terms of sorptivity and dispersion coefficients.

Significance and Impact

The theory derived describes rapid early-time water movement into air-filled fractures in sedimentary rock. Both theory and observations indicate that fractures significantly increase spontaneous imbibition and dispersion of the wetting front in unsaturated sedimentary rocks. Capillary action appears to be supplemented by surface spreading on rough fracture faces. The findings can be applied in modeling hydraulic fracturing.

Research Details

Imbibition into unsaturated Berea sandstone cores was controlled with a Mariotte bottle setup. Images were collected using dynamic neutron radiography and analyzed using ImageJ.

Cheng C. -L., Perfect E., Donnelly B., Bilheux H. Z., Tremsin A. S., McKay L. D., DiStefano V. H., Cai J. C., Santodonato L. J., Rapid imbibition of water in fractures within unsaturated sedimentary rock. 2015.
Advances in Water Resources, Volume 77, Pages 82–89 <http://dx.doi.org/10.1016/j.advwatres.2015.01.010>

Neutron Computed Tomography Characterizes Particulate Properties During Regeneration

Diesel particulate filters (DPF) clean exhaust and reduce pollution

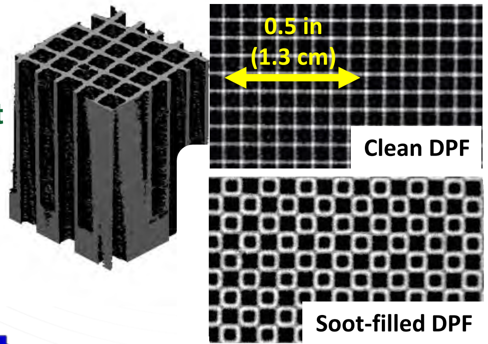

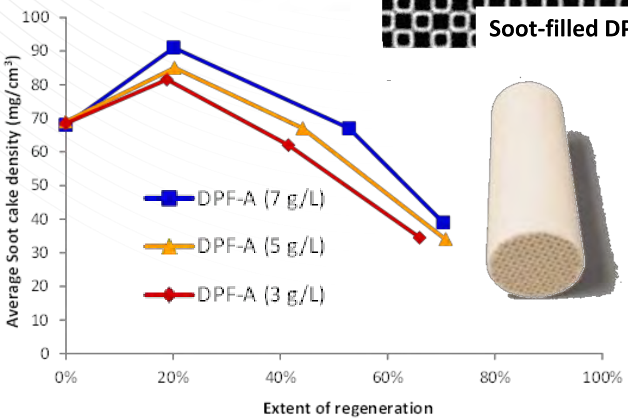

DPFs collect soot during engine operation, leading to soot cake. During regeneration soot cake properties change significantly as identified in neutron imaging campaign.

Work performed at the High Flux Isotope Reactor Imaging (CG1D) beamline was supported by Scientific User Facilities Division, Office of Basic Energy Sciences, US Department of Energy.

T. J. Toops, H. Bilheux, S. Voisin, J. Gregor, L. Walker, A. Strzelec, C. E. A. Finney, J. A. Pihl, Nuclear Instruments and Methods in Physics Research Section A 729 (2013) 581-588.

T. J. Toops, J. A. Pihl, C. E. A. Finney, J. Gregor, H. Bilheux, Emission Control Science and Technology 1:1 (2015) 24-31.

Scientific Achievement

Employed neutron tomography to measure the properties of soot cake layer thickness and subsequently density during a sequential regeneration. Identified key parameters that will aid understanding of the fuel-consuming regeneration process.

Significance and Impact

Understanding the regeneration progression of DPFs is important in improving the efficiency of the process and to understand the correlation between pressure drop and soot level. The results from this work can directly provide model parameters to industry so they can better predict the level soot/particulate in the DPFs.

Research Details

- DPFs were filled to different levels (3, 5 and 7 g/L) using diesel engine
- Full DPFs analyzed with neutron tomography to determine the soot cake thickness and packing density
- Soot cake density, thickness and axial profile measured during sequential regeneration
- Highest soot cake density observed during initial 20% regeneration; layer then loses density, porosity increases and channels open up
- Different soot loading displayed same behavior during regeneration

Biological and Environmental Applications

Neutron Radiography of Roots at CG1-D

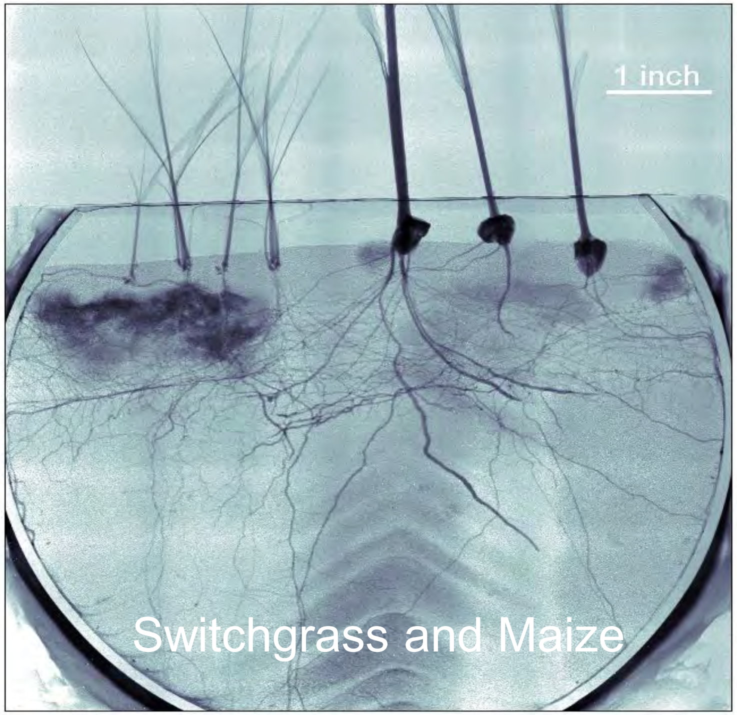

- Water injected into root zone at base
- Unidentified endophyte (symbiotic) or decomposer fungi visible near roots of switchgrass (left), revealing substantial hydration of the rhizosphere
- Both fine and coarse roots are readily visible

J. Warren (PI), H, Bilheux, M. Kang, S. Voisin, C. Cheng, J. Horita, E. Perfect, Plant Soil, 2013

Investigating novel contrast agents for biological applications

- Observation of water fluxes in soil/root surrounded with fungi is challenging due to lack of contrast between fungi and water
  - Unlike heavy water (D_2O) which provides a lesser image contrast, the use of Gd compounds as tracers provide a strong neutron attenuation (i.e. contrast) that can be followed as a function of time in a plant system.
  - Gd-compounds are good candidates to serve as tracers for solid movements – possible use as a tracer for nutrients (e.g. phosphorus, nitrogen).
  - Gd-based MRI contrast agents prepared as a liquid solution (0.25-1M concentration) were hydroponically fed to plants prior to conducting the imaging experiments.
  - Toxicity of Gd compounds will need to be evaluated through time.

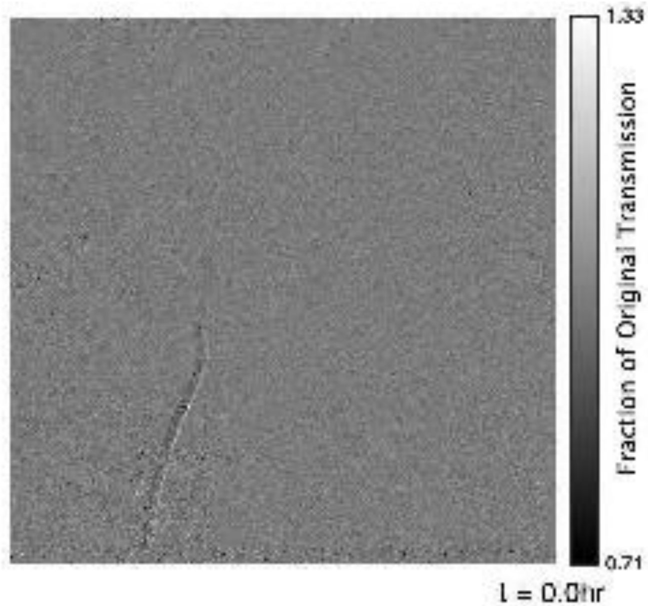

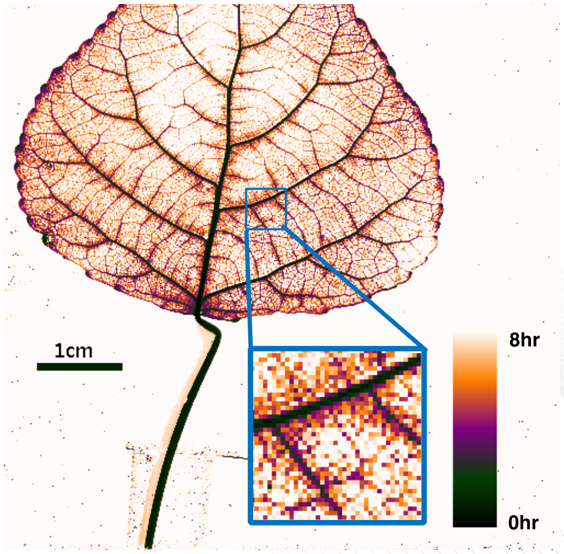

Courtesy of DeCarlo K., Jacobson S., Bilheux, (2017).

Oak Ridge National Laboratory

Changes in Soil and Root Water Content using Neutron Radiography

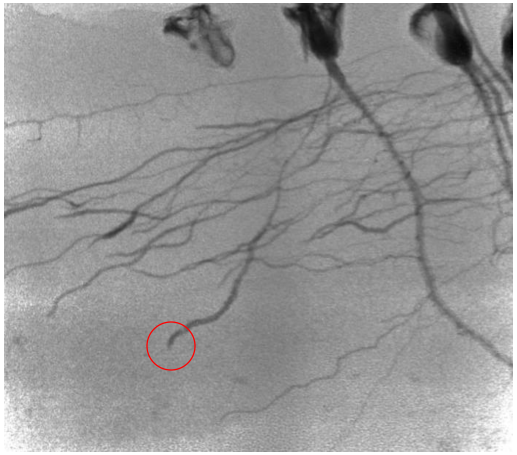

t = 0 h

t= 12 h

t= 12/t= 0

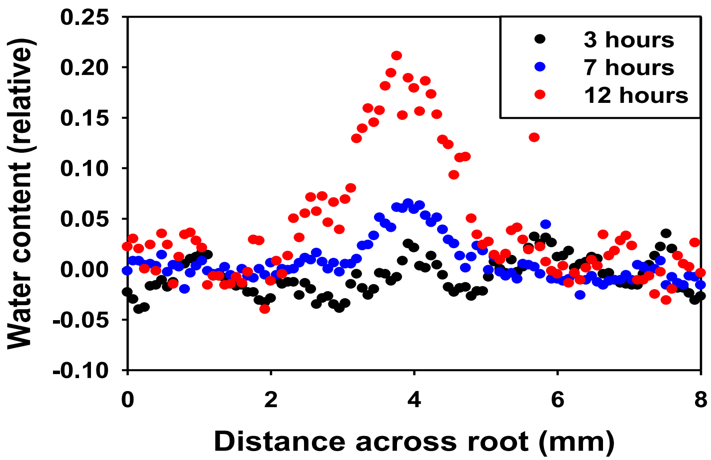

Top – More water showing up based on division (white areas)

Blue arrows show where water was removed from the system.

Left – increase in water content or root or rhizosphere due to root growth or root water efflux

J. Warren (PI), H, Bilheux, M. Kang, S. Voisin, C. Cheng, J. Horita, E. Perfect, Plant Soil, 2013

Neutron sensitivity to H atoms and thus observe Water Uptake by Roots and Stem

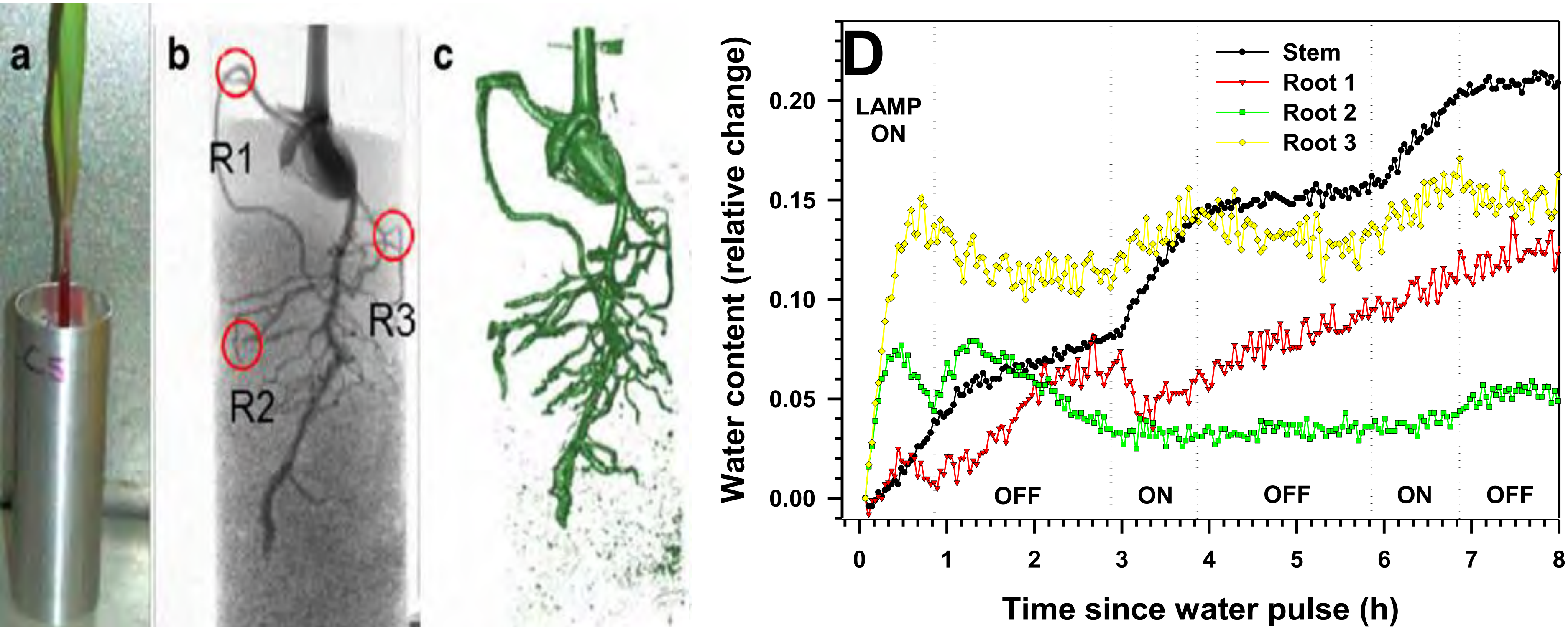

10-d old maize seedling (A) aluminum sample chamber; (B) neutron radiograph at ~70 µm pixel resolution illustrating roots distribution (0.2-1.6 mm); C) 3D tomographic reconstruction; (D) Timing of water uptake by plant components highlighted in (B) illustrating impact of solar radiation on rate of water flux in stem and ~0.5 mm first and second order roots.

- <u>This study provides direct evidence for root-mediated hydraulic redistribution of soil water to rehydrate drier roots</u>

Plant Soil, 2013, DOI 10.1007/s11104-012-1579-7

MRI, X-CT, and NR imaging techniques

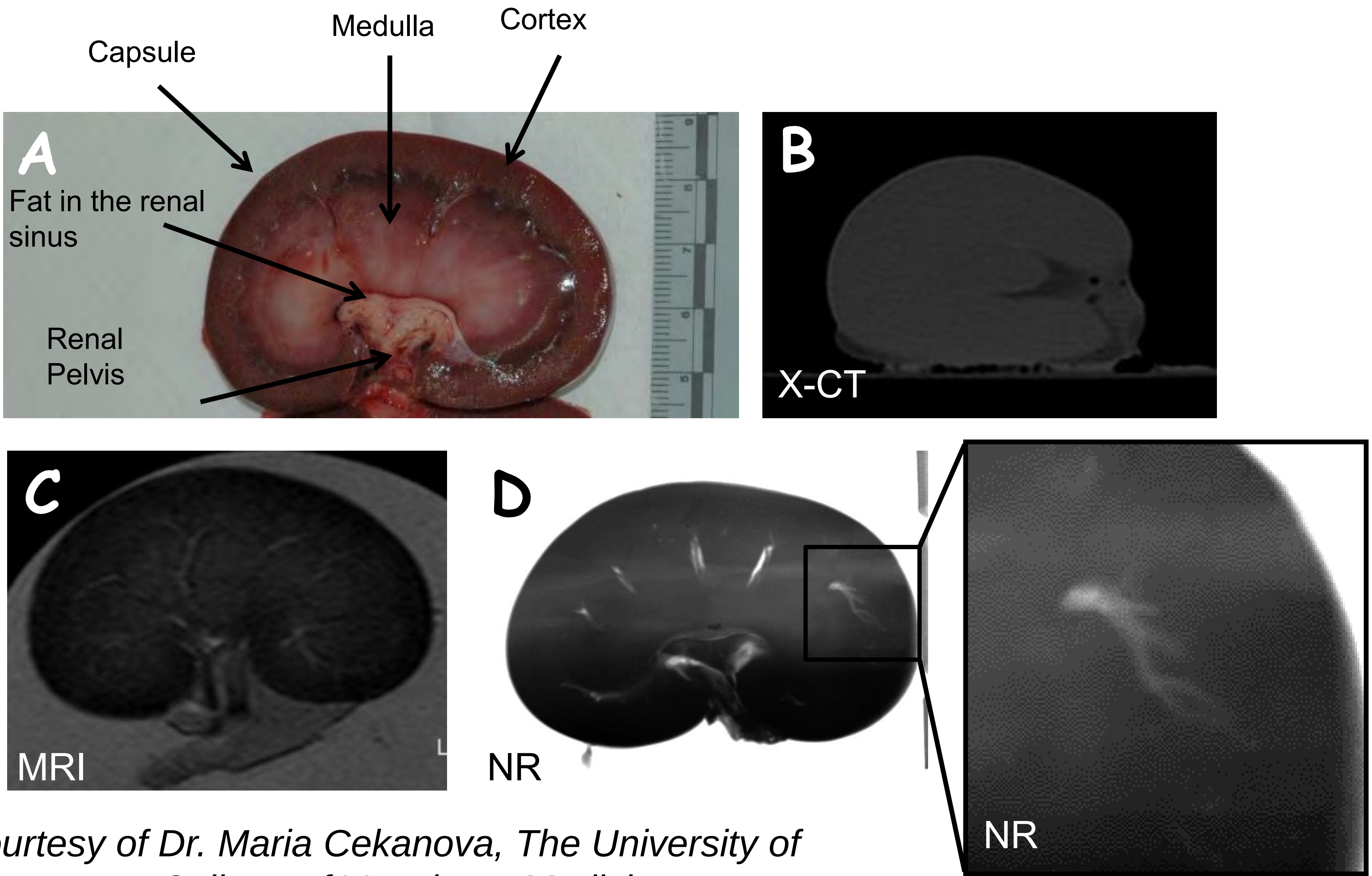

Courtesy of Dr. Maria Cekanova, The University of Tennessee, College of Veterinary Medicine

A novel approach to determine post-mortem interval using neutron radiography

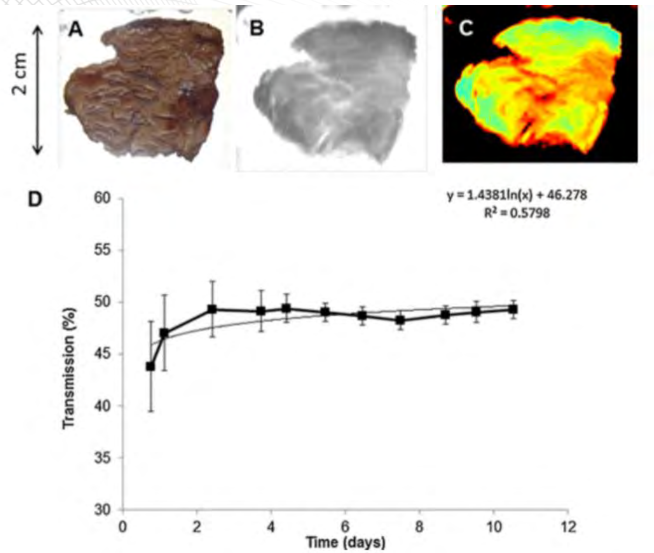

(A) Photograph, (B) gray scale and color enhanced (C) neutron radiograph of a 2 cm × 2 cm × 1 mm thick skeletal muscle tissue. (D) Neutron transmission as a function of time of skeletal muscle tissues under controlled conditions with natural logarithm fit.

H. Z. Bilheux , M. Cekanova, A. A. Vass, T. L. Nichols, J. C. Bilheux, V. Finochiarro, **Forensic Science International**, doi:10.1016/j.forsciint.2015.02.017 (March

Work performed at ORNL's High Flux Isotope Reactor CG-1D and Spallation Neutron Source VULCAN beamlines was supported by Scientific User Facilities Division, Office of Basic Energy Sciences, US Department of Energy. Part of this research sponsored by NIJ.

Scientific Achievement

PMI was objectively estimated by measuring changes in neutron transmission correlated with H content variation in decaying tissues.

Significance and Impact

- One of the most difficult challenges in forensic research for criminal justice investigations is to objectively determine post-mortem interval (PMI).
- The estimation of PMI is often a critical piece of information for forensic sciences.
- Most PMI techniques rely on gross observational changes of cadavers that are subjective to the forensic anthropologist.

Research Details

- Tissues exposed to controlled (laboratory settings) and uncontrolled (University of Tennessee Anthropology Research Facility) environmental conditions.
- Neutron radiographs were compared to histology data to assess the decomposition stage
- Over a period of 10 days, changes in neutron transmission through lung and muscle were found to be higher than bone by 8.3%, 7.0%, and 2.0%, respectively.

A novel approach to determine post-mortem interval using neutron radiography (cont'd)

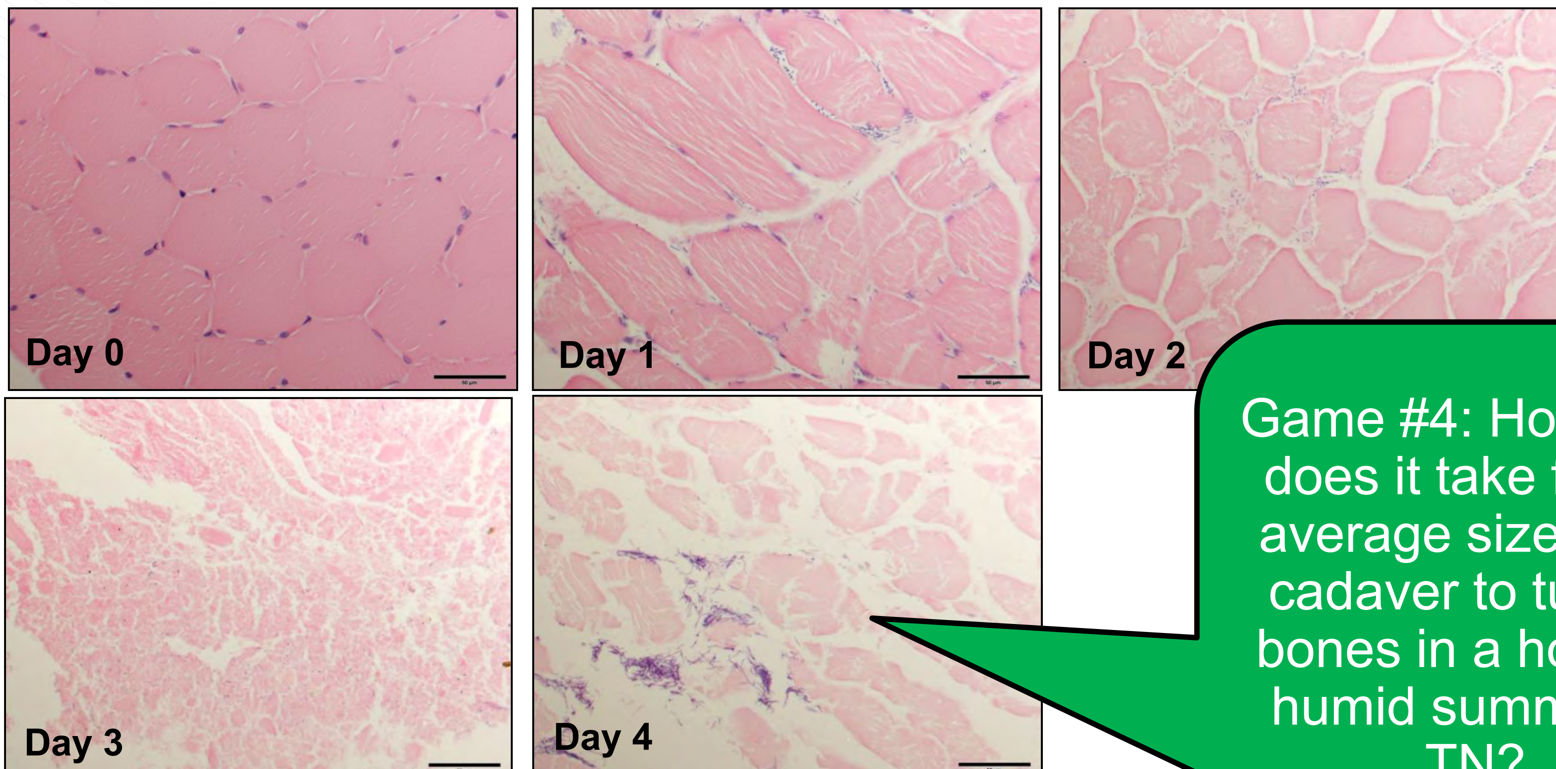

Game #4: How long does it take for an average size adult cadaver to turn to bones in a hot and humid summer in TN?

Acknowledgments

- Research sponsored by the **Laboratory Directed Research and Development Program** of Oak Ridge National Laboratory, managed by UT-Battelle LLC, for DOE.
- Resources at the **High Flux Isotope Reactor (HFIR) and Spallation Neutron Source (SNS)**, U.S. DOE Office of Science User Facilities operated by ORNL, were used in this research.
- Research at **Manufacturing Demonstration Facility (MDF)** was sponsored by the U.S. Department of Energy, Office of Energy Efficiency and Renewable Energy, Advanced Manufacturing Office, under contract DE-AC05-00OR22725 with UT-Battelle, LLC.
- Thanks to J. Molaison, M. Frost and H. Skorpenske for setting up the detector and furnace at the SNS beamlines.

Thank you

(bilheuxhn@ornl.gov)

Courtesy of
Prof. Krysta Ryzewski, Wayne University
Susan Herringer, Prof. Brian Sheldon, Brown University

OAK RIDGE National Laboratory